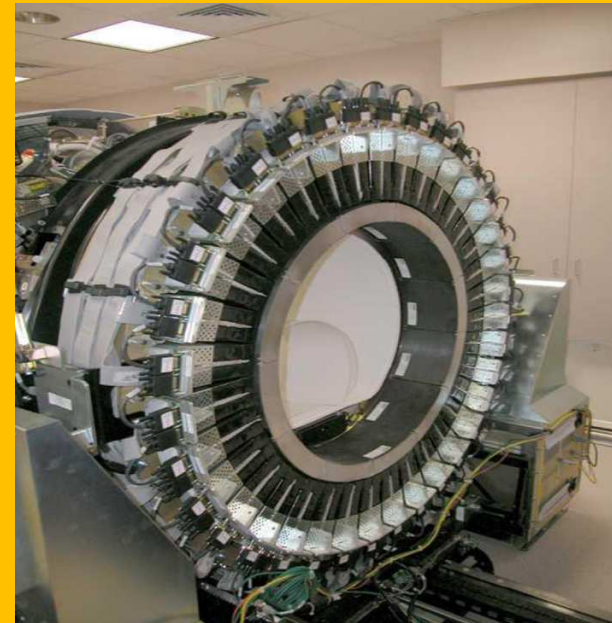
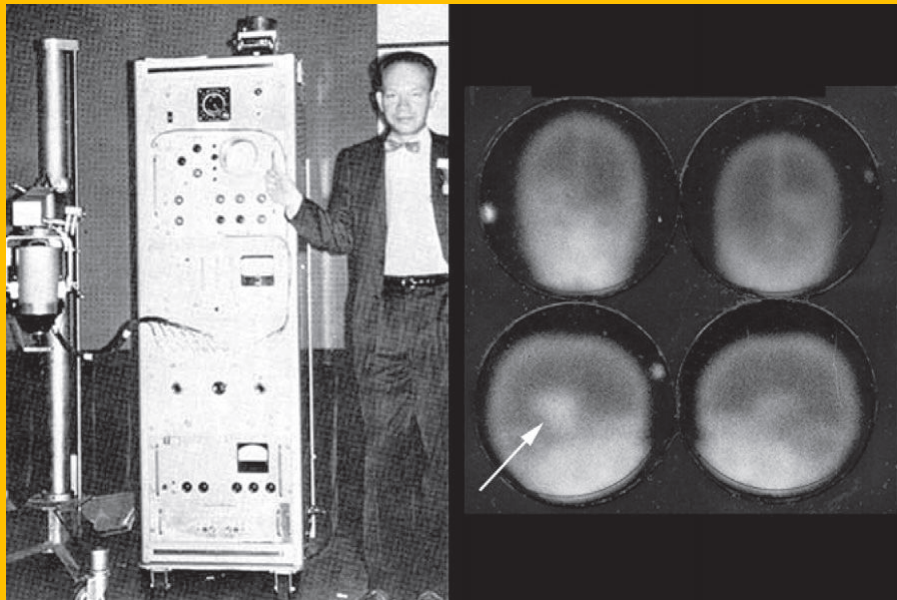
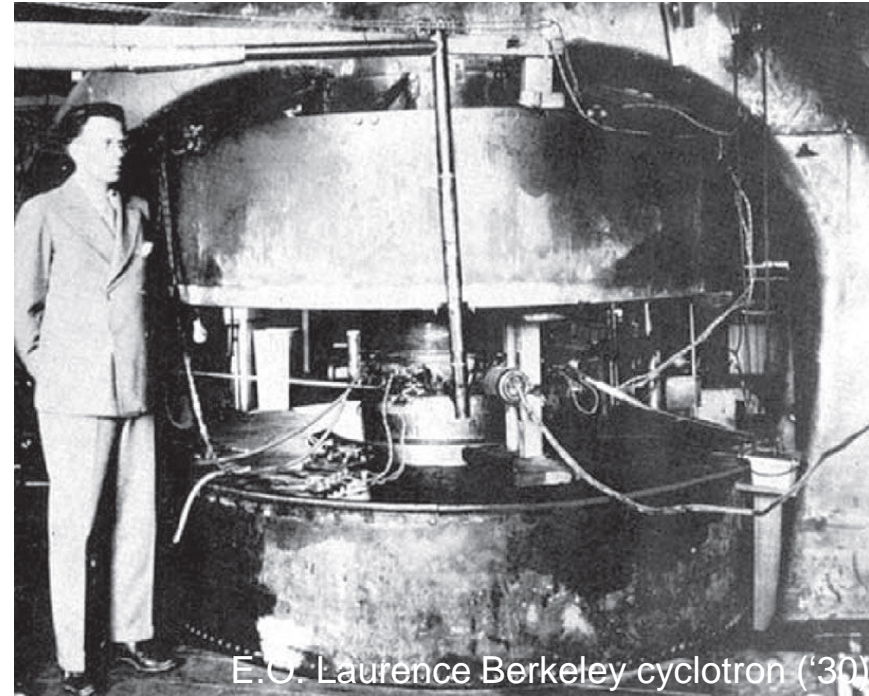
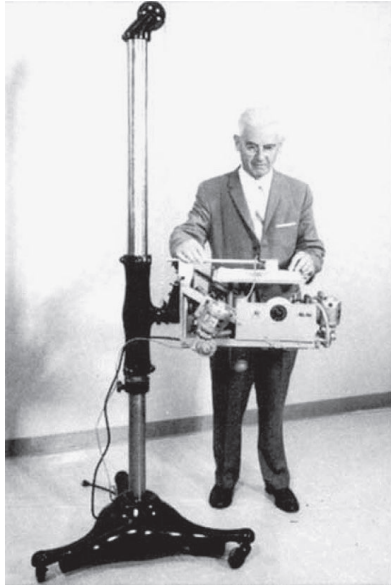


Medical Imaging techniques (SPECT and PET)

S. Gnesin

Institute of Radiation Physics, Lausanne University Hospital, Lausanne, Switzerland

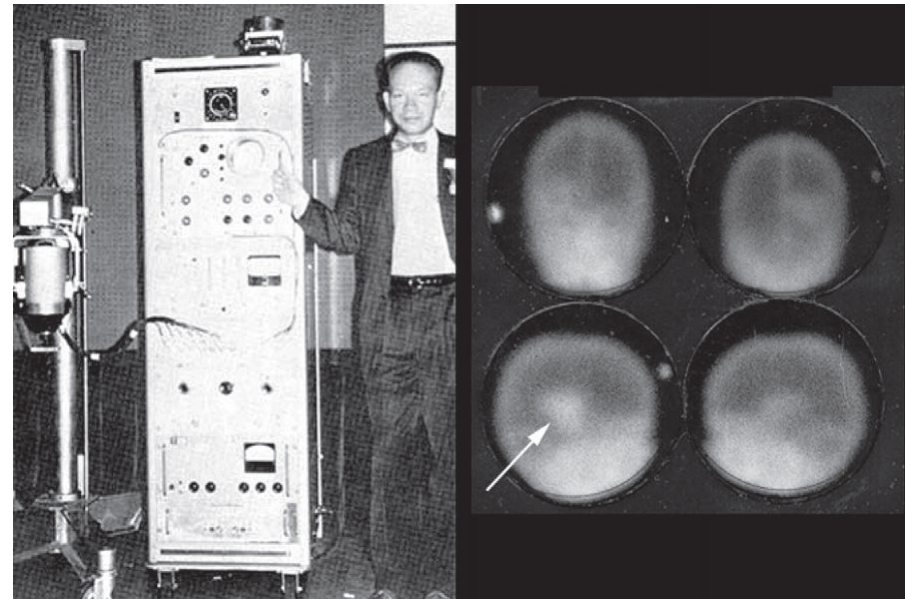




E.O. Lawrence Berkeley cyclotron ('30)

Rectilinear scanner 1951
 Simple scintillator counter
 I-131 Thyroid
 Planar imaging
 Ink intensity is proportional
 To measured photon count-rate

H. Anger 1958
 First Gamma Camera
 Tc-99m Pertechnetate
 Brain scan of a patient with a glioma



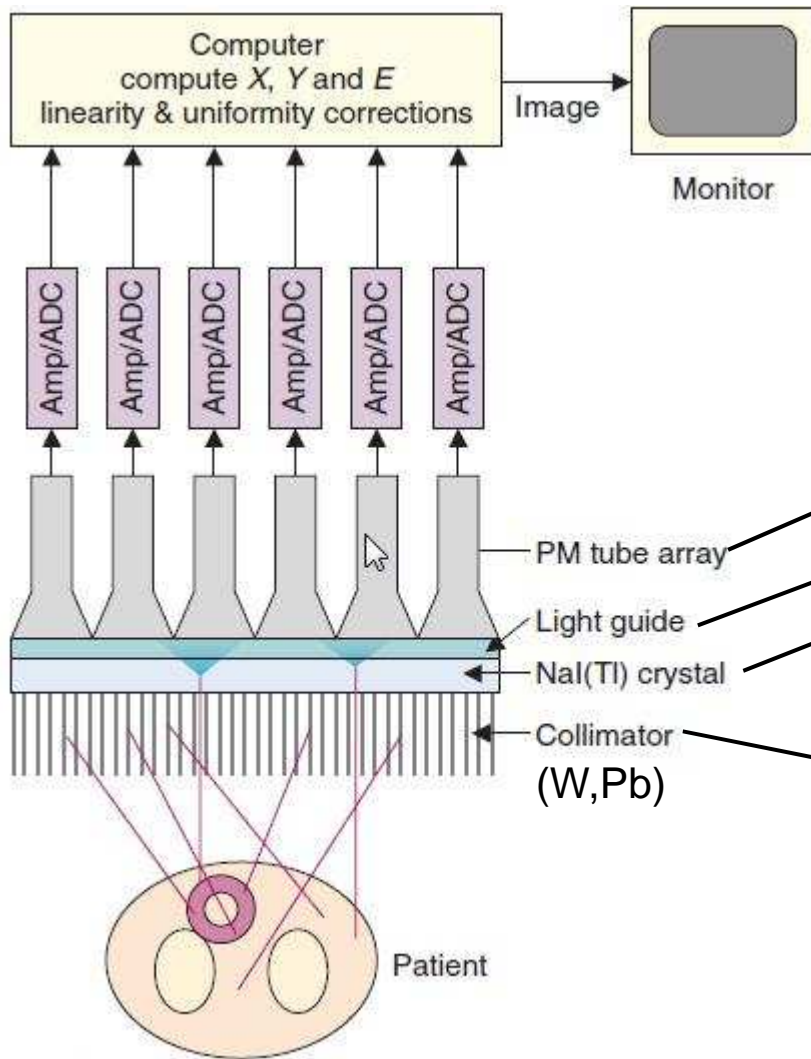
Which devices

- **Imaging devices**

- Gamma camera
- SPECT/CT
- PET/CT (PET/MRI)

Gamma Camera

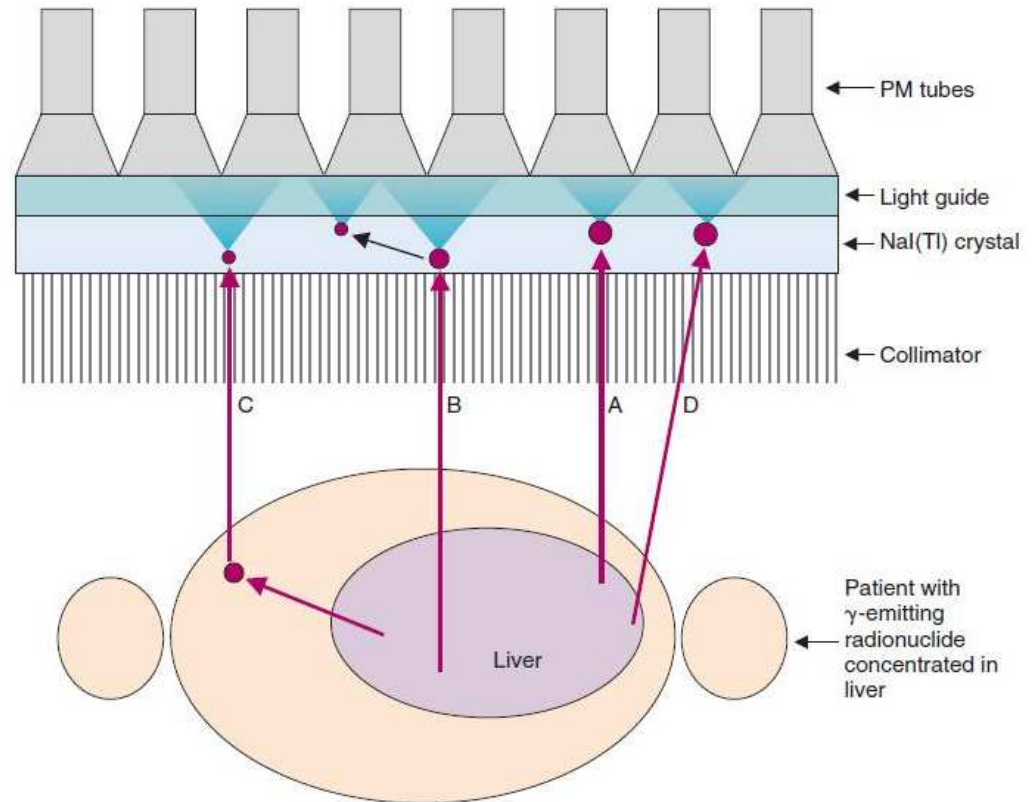
Gamma camera: main components



- Emission imaging is based on scintillation detection
- Line of sight are defined by collimation (W or Pb collimator)



Gamma camera: Problems in event localization



A) Valid event (useful for correct localization on the imaged region)

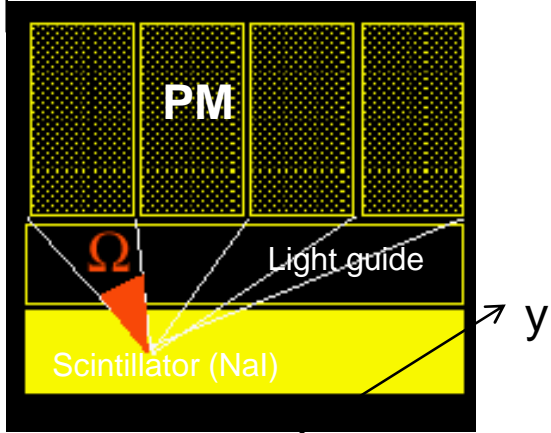
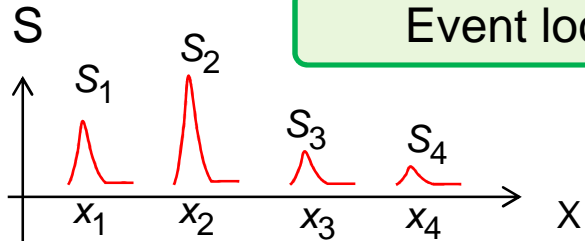
B) Scatter on the crystal

C) Scatter on the patient

D) Septal penetration

} Incorrect source localization

Event localization on the crystal surface



Centroid (baricenturm) of the PM response

$$x = \frac{\sum_{i=1}^n S_i x_i}{\sum_{i=1}^n S_i}$$

$$y = \frac{\sum_{i=1}^n S_i y_i}{\sum_{i=1}^n S_i}$$



Software positioning also account for non-linearity
In PM response

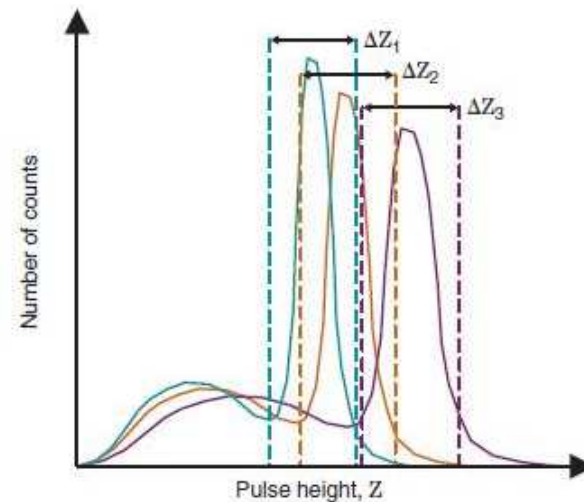
Pulse height analysis and energy determination

Discriminate gamma events

Scattered photons

Threshold level on signal height
→ Acceptance energy window
(photoelectric peak)

No scatter (or low scatter) is accepted
for image formation

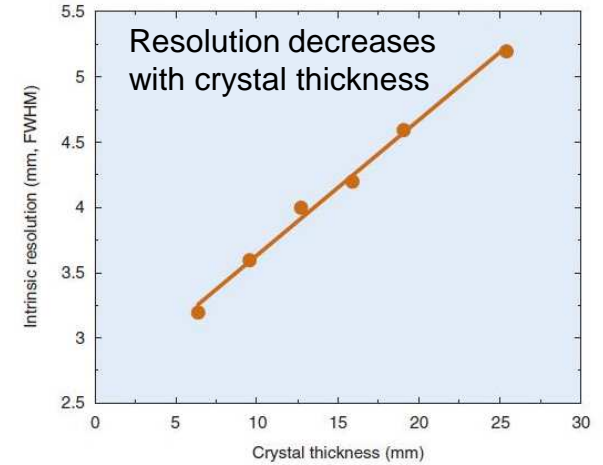
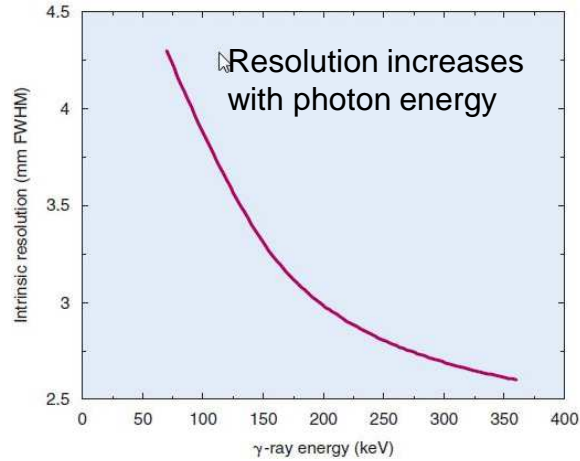


Gamma camera: Performances

Intrinsic spatial resolution (detector)

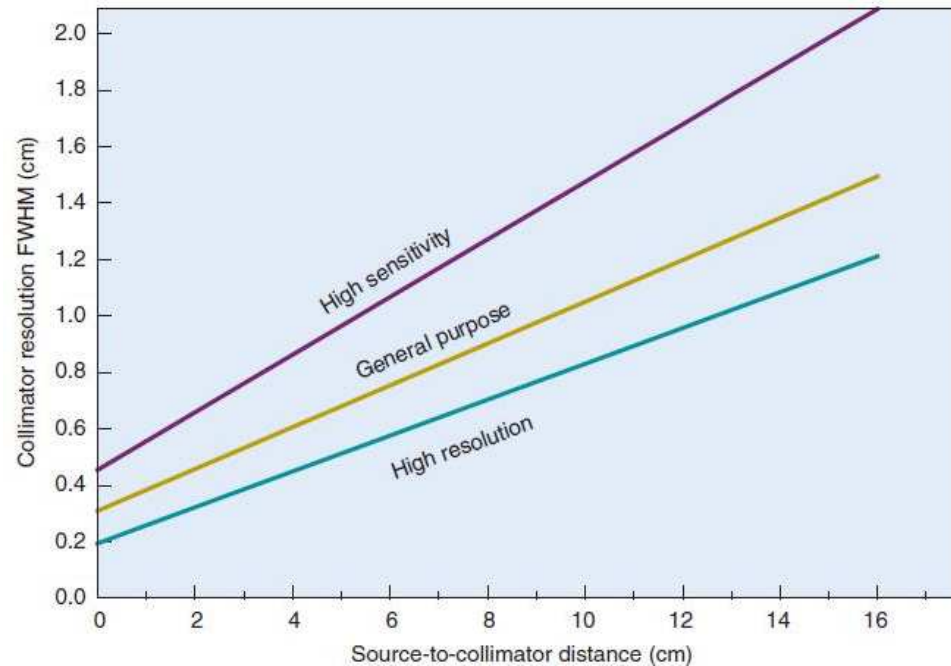
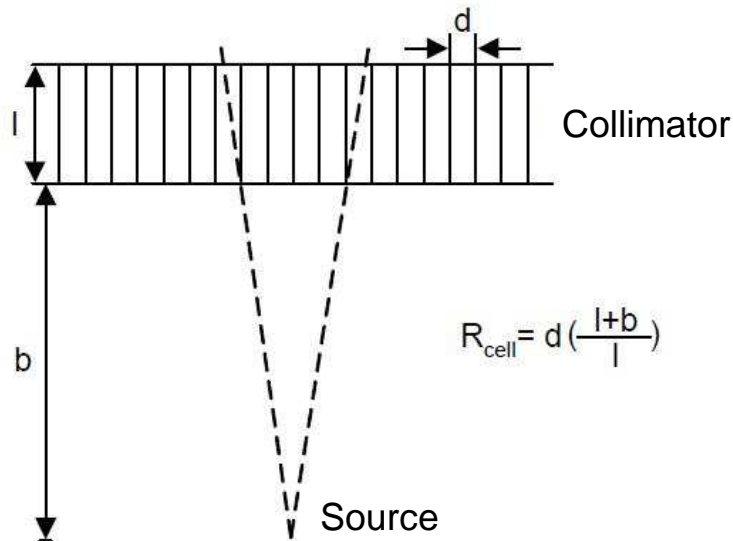
→ (4mm)

- Impinging gamma energy
- Crystal thickness



Collimator resolution (parallel-hole)

~10 mm



Gamma camera Sensitivity

Collimator Efficiency

$$S_{coll} = \frac{\Omega}{4\pi} \frac{A_{holes}}{A_{crystal}} = \frac{\pi \left(\frac{d}{2}\right)^2 / l^2}{4\pi} \frac{A_{holes}}{A_{crystal}}$$

Ω : solid angle subtended by the collimator hole from the source
 d : collimator hole diameter
 l : collimator length (septa length)

Total Efficiency

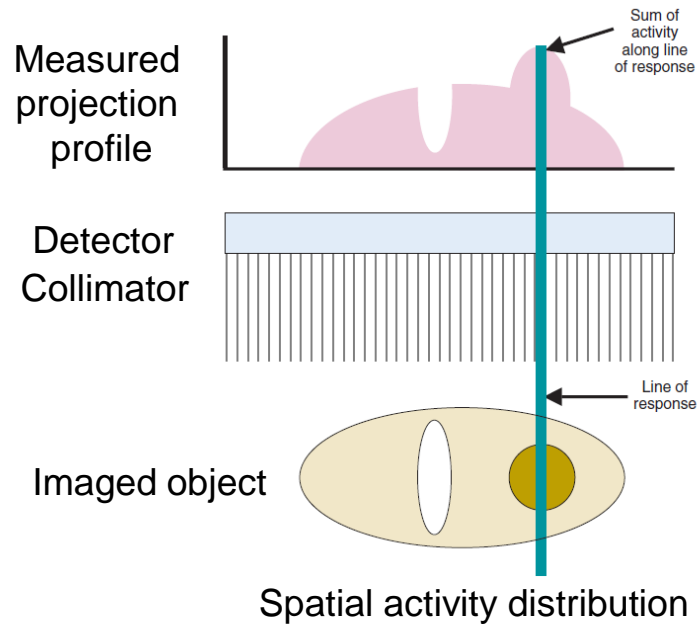
$$S_{tot} = \left[\frac{\Omega}{4\pi} \frac{A_{holes}}{A_{crystal}} \right] \times \left[1 - e^{-\mu d_{crystal}} \right]$$

Detection efficiency
(crystal)

Collimator Type	Recommended Max. Energy (keV)	Efficiency, g	Resolution R_{coll} (FWHM at 10 cm)
Low-energy, high-resolution	150	1.84×10^{-4}	7.4 mm
Low-energy, general-purpose	150	2.68×10^{-4}	9.1 mm
Low-energy, high-sensitivity	150	5.74×10^{-4}	13.2 mm
Medium-energy, high-sensitivity	400	1.72×10^{-4}	13.4 mm

Tomographic reconstruction

Bases of tomography reconstruction in nuclear medicine

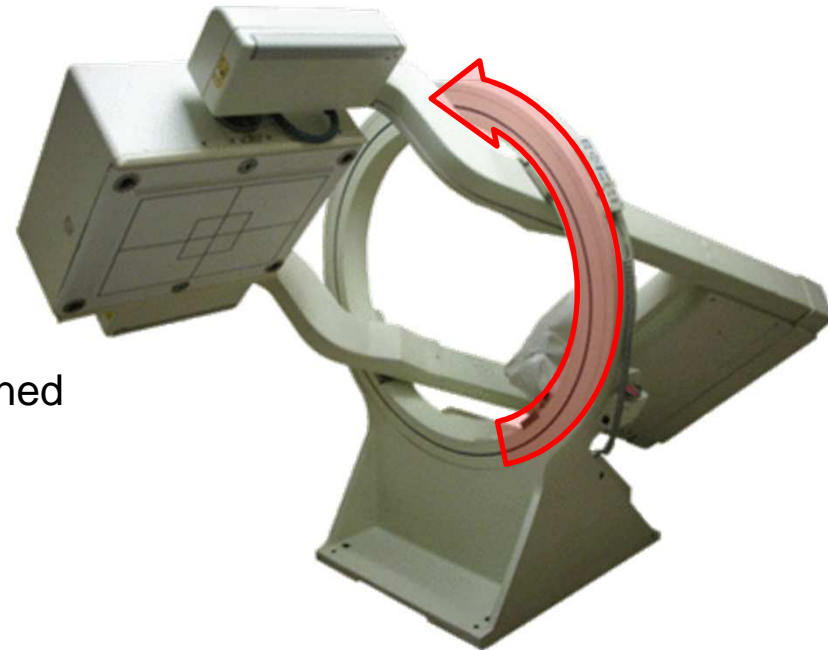


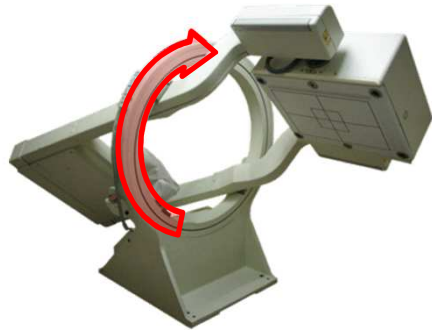
Projections in a simple 1-D detector case

Signal proportional to the summed activity along the line of response
(assumption of no attenuation and scatter)

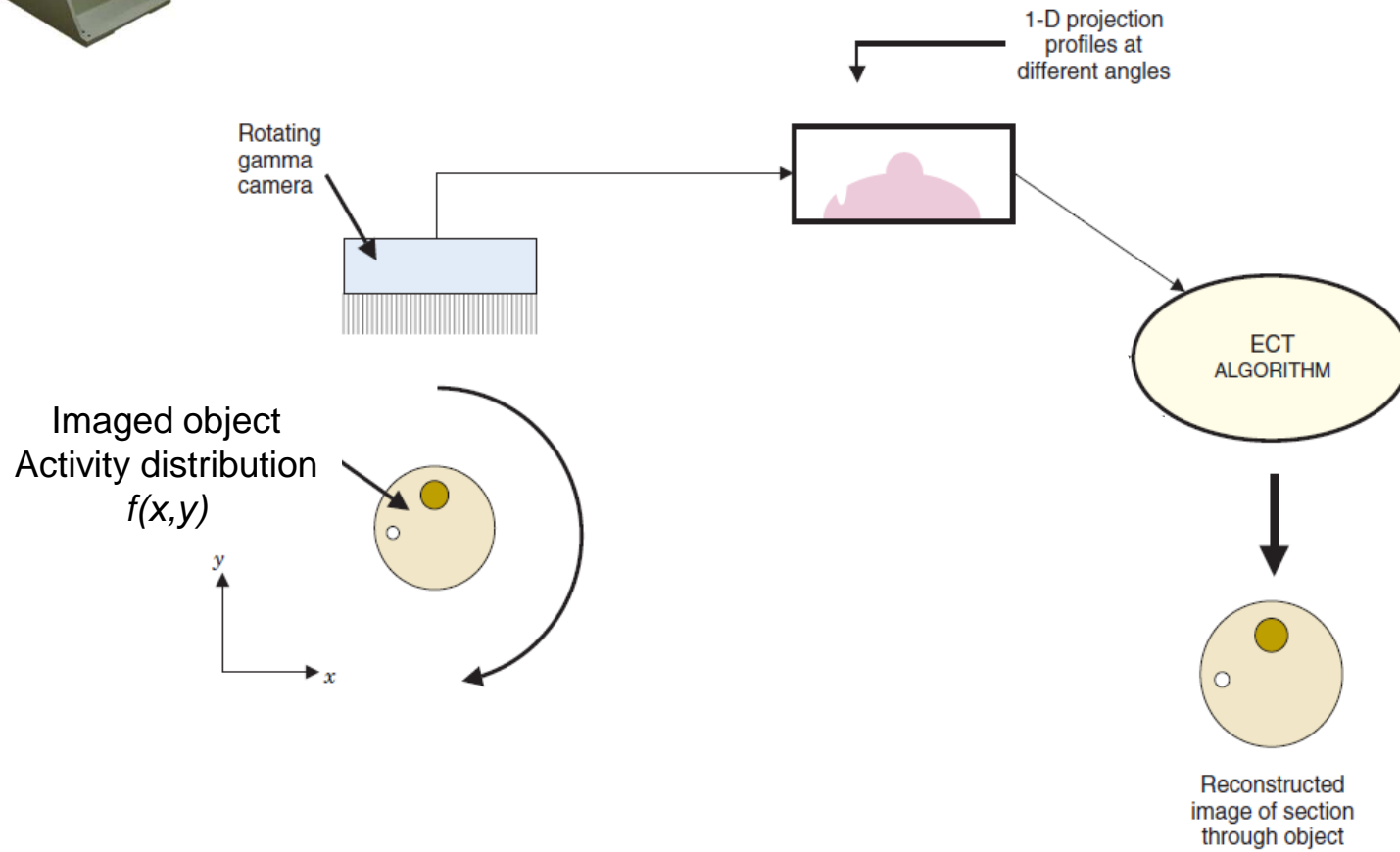
Head rotation around the imaged object

Many projections at different angles are obtained

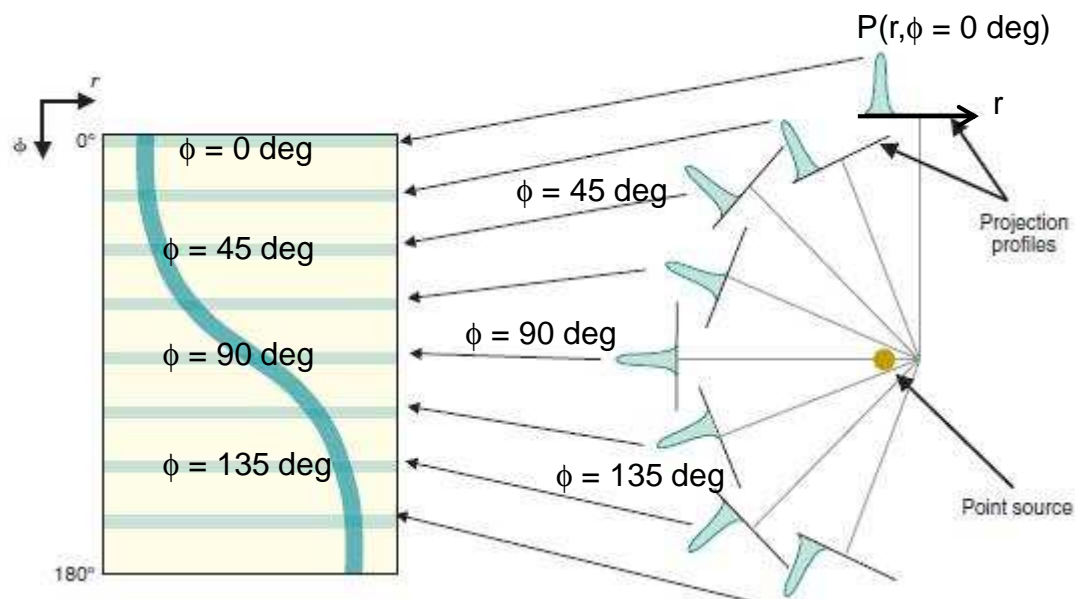




1-D projections of a unknown activity distribution $f(x,y)$

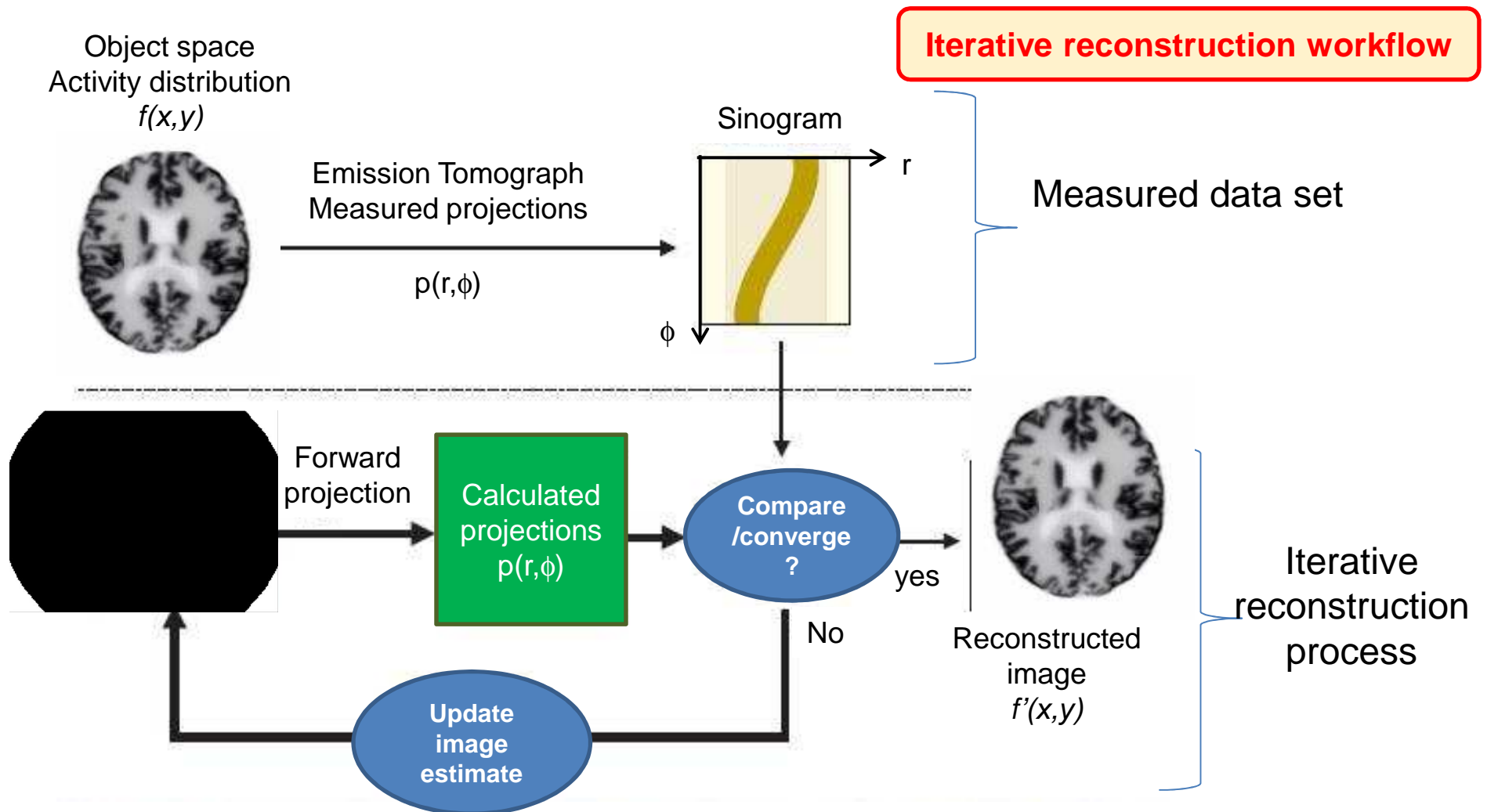


N projections $p(r,\phi)$ \longleftrightarrow N angular samples \longleftrightarrow N sinogram lines in the (r,ϕ) space



1-D Projection data are arranged in a
2D (r,ϕ) **SINOGRAM** representation

Each row (ϕ) in the sinogram displays the intensity profile
measured in the corresponding projection

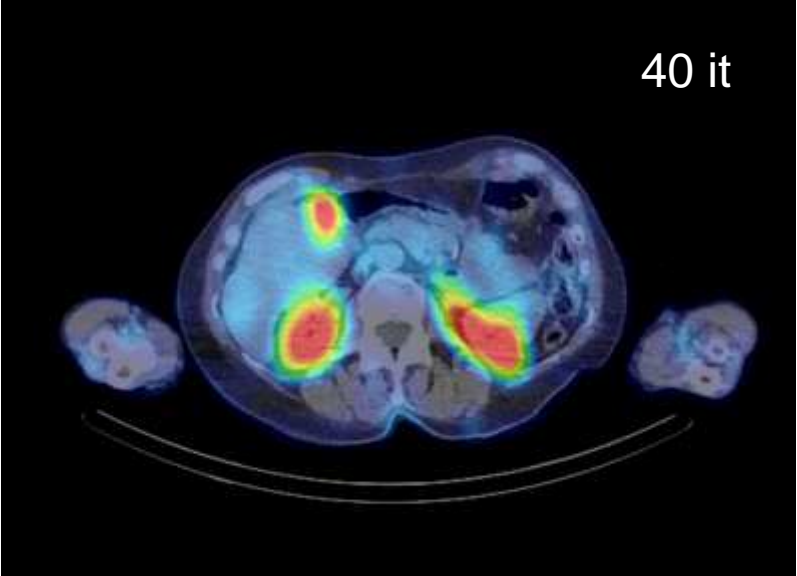


Expectation maximization cost function
(convergence criterion)

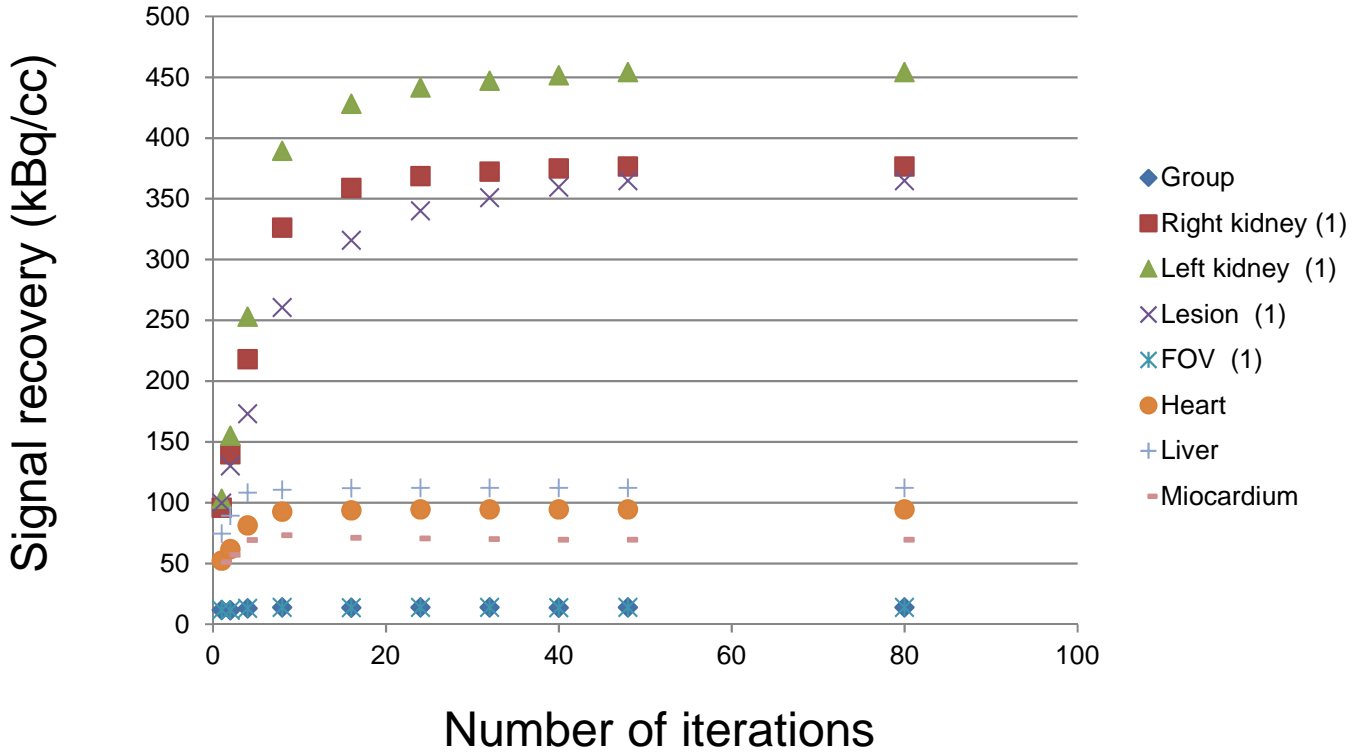
$$f_i^{k+1} = \frac{f_i^k}{\sum_{j=1}^m M_{i,j}} \times \sum_{j=1}^m M_{i,j} \frac{p_j}{\sum_{i'=1}^n M_{i',j} f_{i'}^k} \quad p_j = \sum_{i=1}^n M_{i,j} f_i$$

Method to upgrade the image estimate
Account for:

- *Detector and collimator response,*
- *finite spatial resolution*
- *Attenuation*
- *Scattering*



- Detection/Localisation
- Contrast
- Quantification

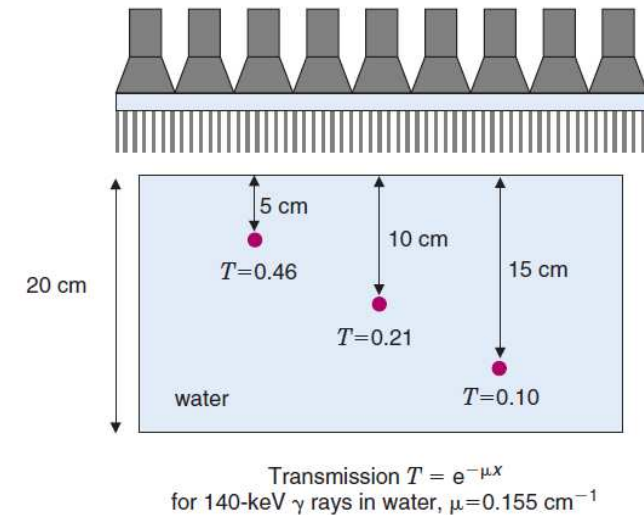
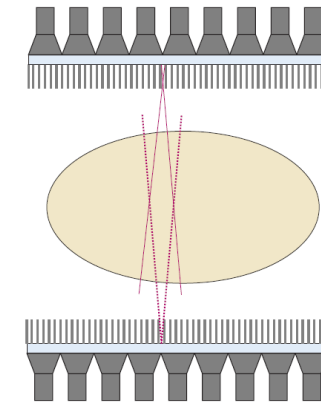
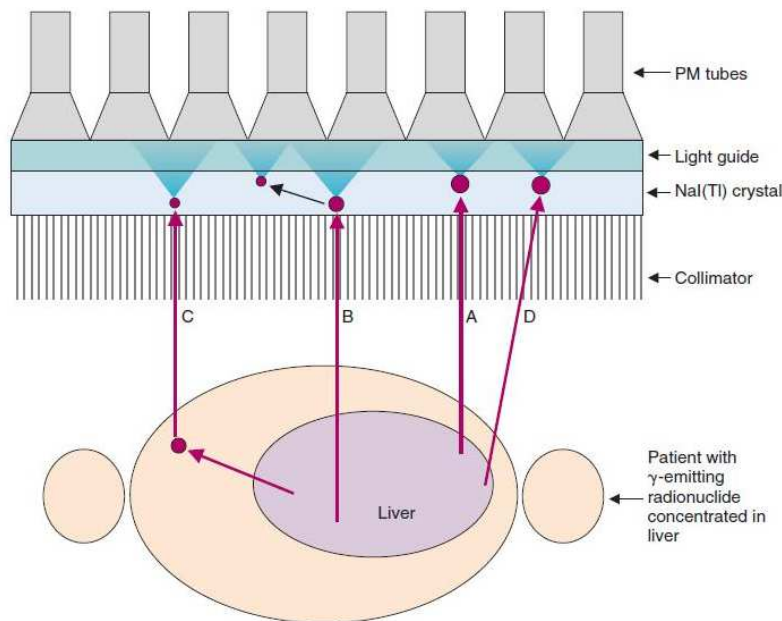


SPECT/CT

Signal intensity in SPECT voxels is proportional to the amount of activity contained

But **absolute quantification (Bq/mL) is very hard to achieve**

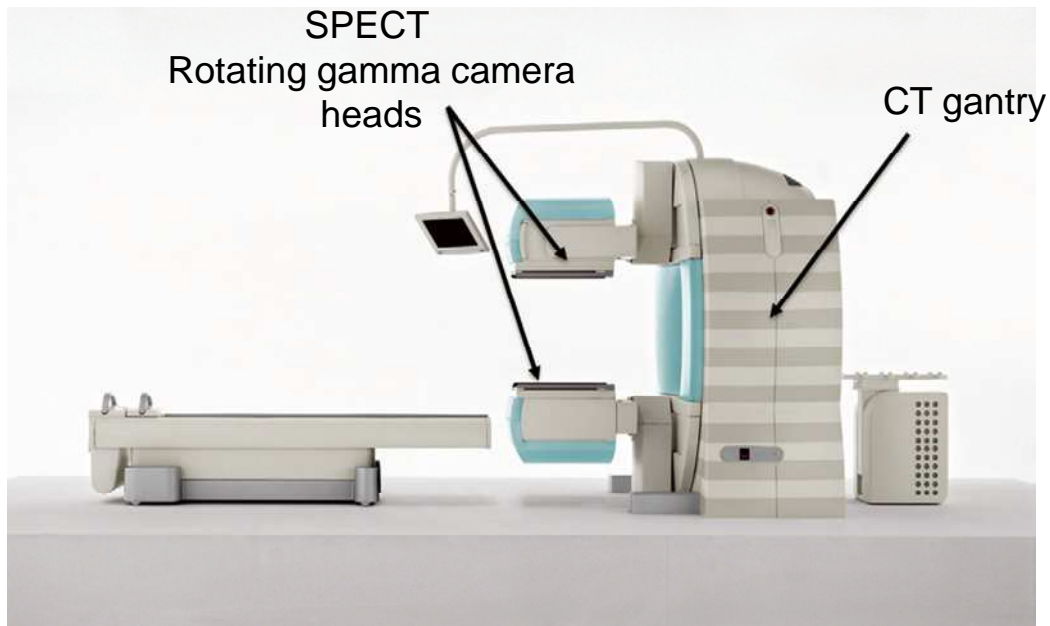
- **Line of response** are not straight cylinders but are diverging cones
- **Tissue attenuation** results in depleted signal from deeper location in patient
- **Scattering** in patient, detector and collimator results in event mislocalisation



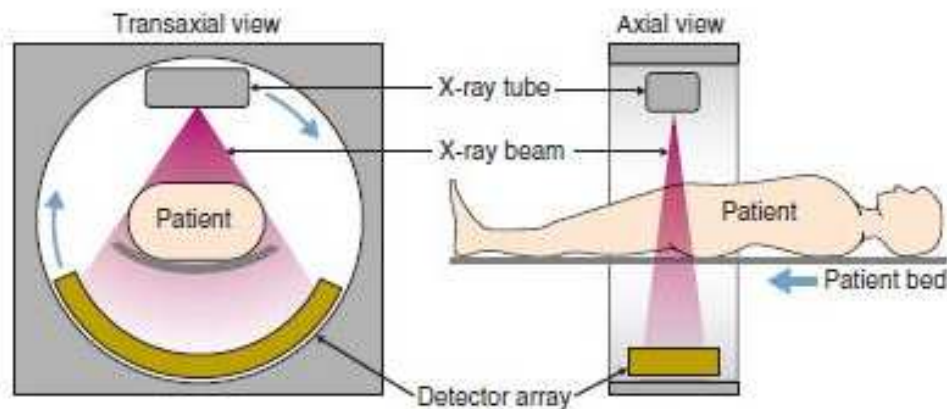
- An exact **detector collimator response** is needed (septal penetration, PSF resolution recovery)

SPECT

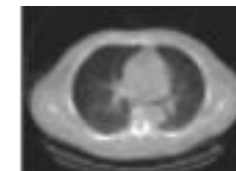
CT based attenuation correction in SPECT



Tissue attenuation can be derived from transmission data (CT)

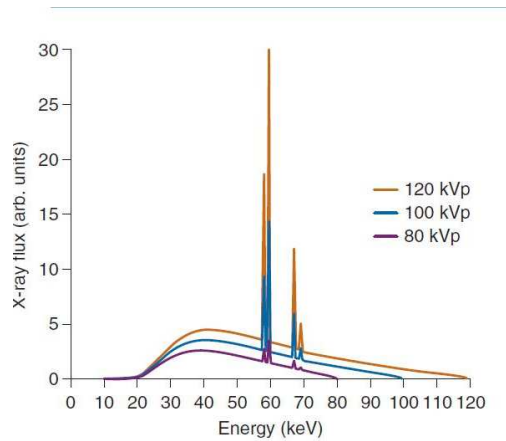


CT-Based
Attenuation map
For attenuation Correction of
SPECT data



CT-AC is standard in modern hybrid SPECT/CT devices

CT based attenuation correction in SPECT



Effective energy of the beam
can be defined

120 kVp \rightarrow 75 keV

Appropriate $\mu(x,y,E_\gamma)$ map need:

Energy scaling the attenuation coeff.
from effective beam energy to the given
radionuclide energy

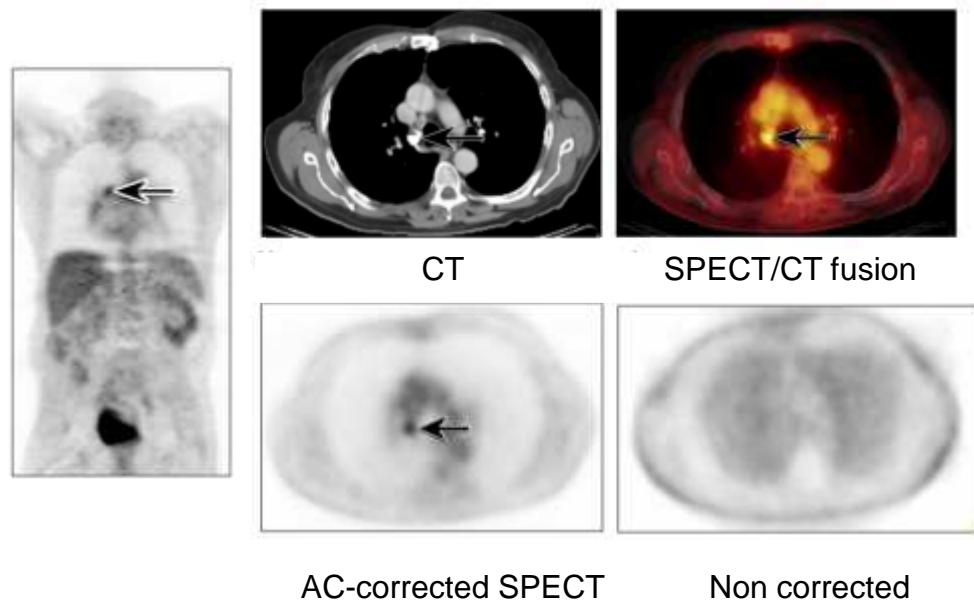
CT map is in Hounsfield units obtained from a broad-energy
Spectrum

Segmentation on CT

- Air
- Bone
- Soft tissues

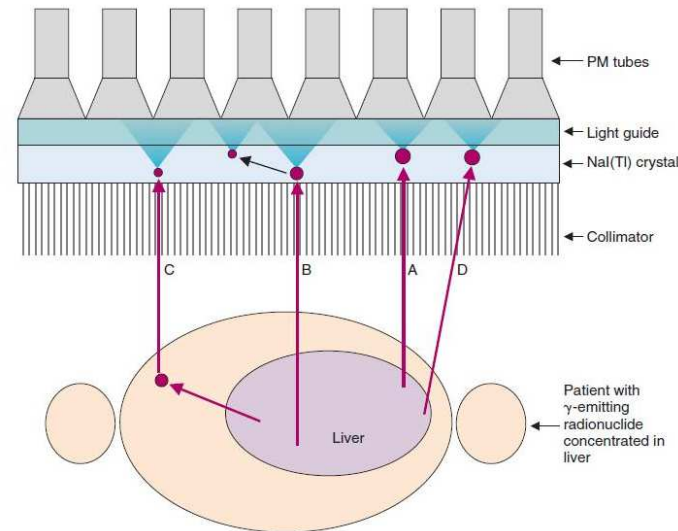
Attenuation map $\mu(x,y,E_\gamma)$

Continuous attenuation map $\mu(x,y,E_\gamma)$ from CT



Scatter correction in SPECT

➤ **Scattering** in patient, detector and collimator results in event mislocalisation



Scatter fraction in the selected energy window in unfavorable condition can be up to 40%

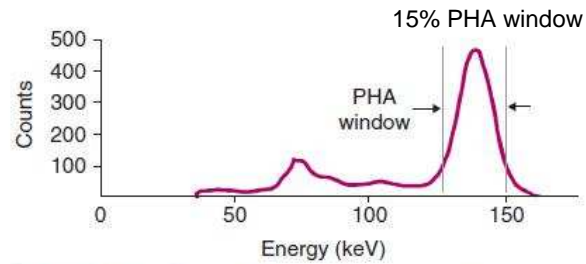
Scatter correction by Chang corrections → smaller attenuation coefficient

Only works in regions of uniform activity distribution and attenuation

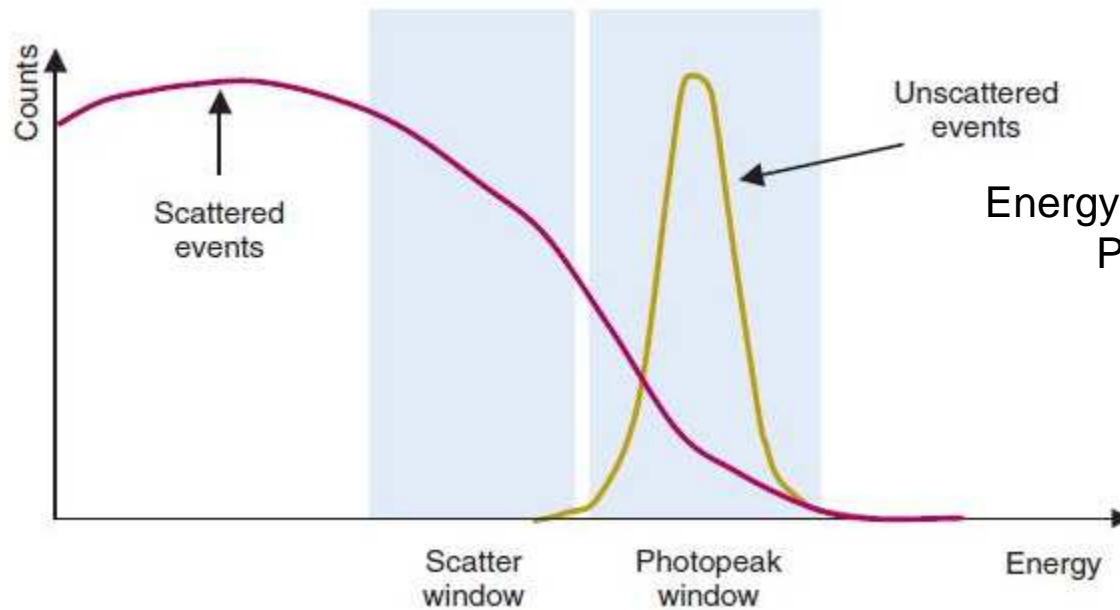
Scatter correction by measured scatter component subtraction in projections

Scatter correction by energy discrimination in PHA

Scatter correction in SPECT PHA based energy discrimination



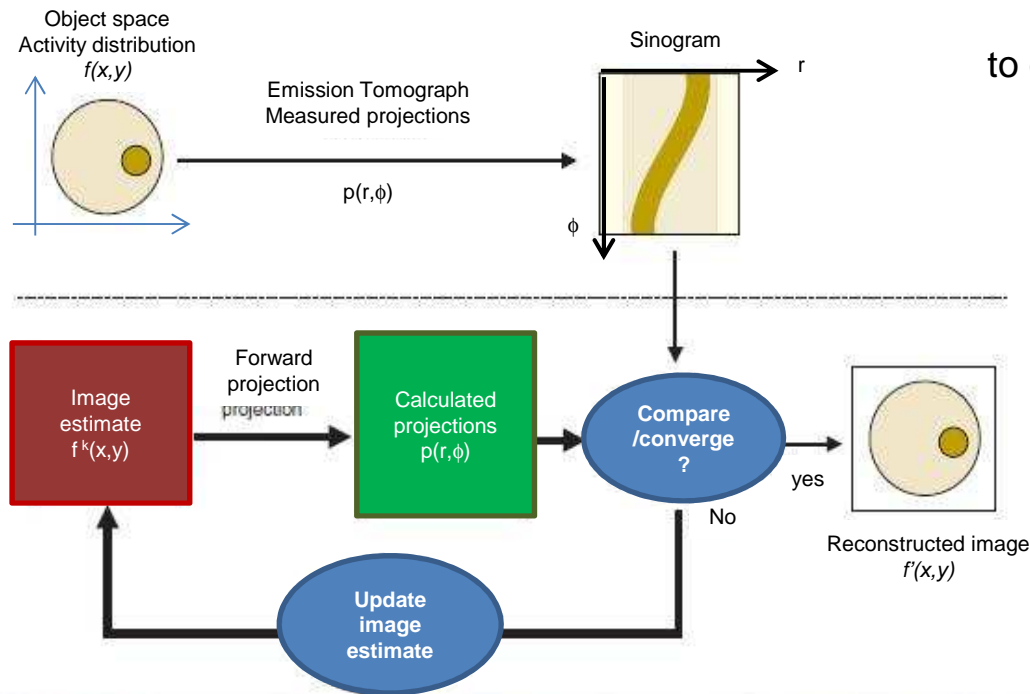
Typical energy spectrum from ^{99m}Tc source
(without attenuating/scattering media)



Energy spectrum in the presence of scattering
Patient (especially obese patients)

Scatter correction must be performed before Attenuation correction
to avoid amplification of scatter contribution

Attenuation and Scatter correction in SPECT Iterative reconstruction



All image pixels (i) have a finite probability ($M_{i,j}$) to contribute to signal intensity into projection data (p_j)

$$p_j = \sum_{i=1}^n M_{i,j} f_i$$

$$f_i^{k+1} = \frac{f_i^k}{\sum_{j=1}^m M_{i,j}} \times \sum_{j=1}^m M_{i,j} \frac{p_j}{\sum_{i'=1}^n M_{i',j} f_{i'}^k}$$

Attenuating map data can be integrated into the Image Matrix (M)

To account for the probability of scatter radiation in the source region (x,y) to produce a signal into a given detector element (p_j)

Collimator/detector response can also be integrated in M

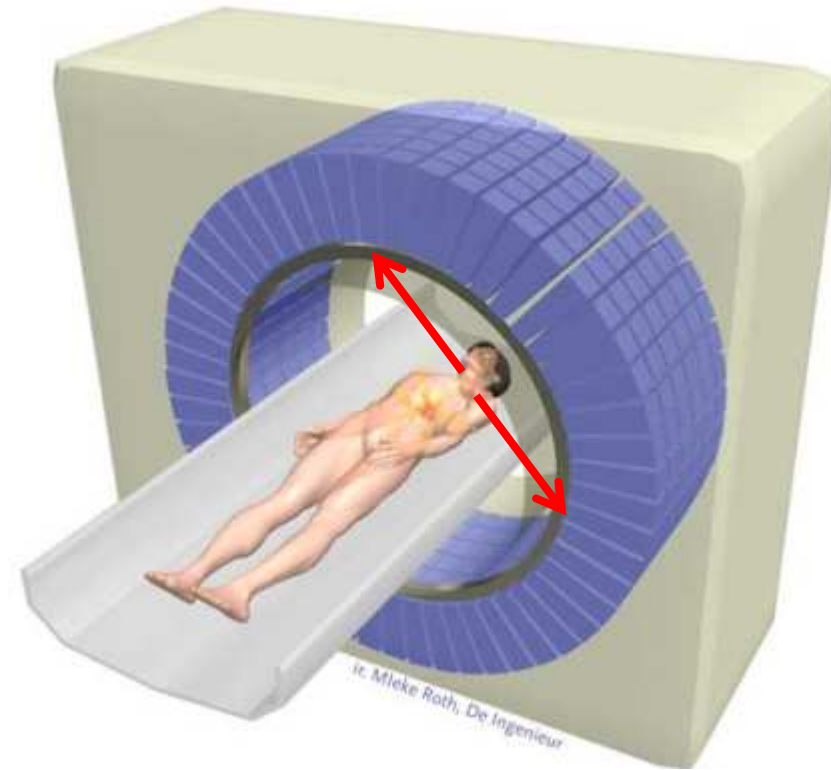
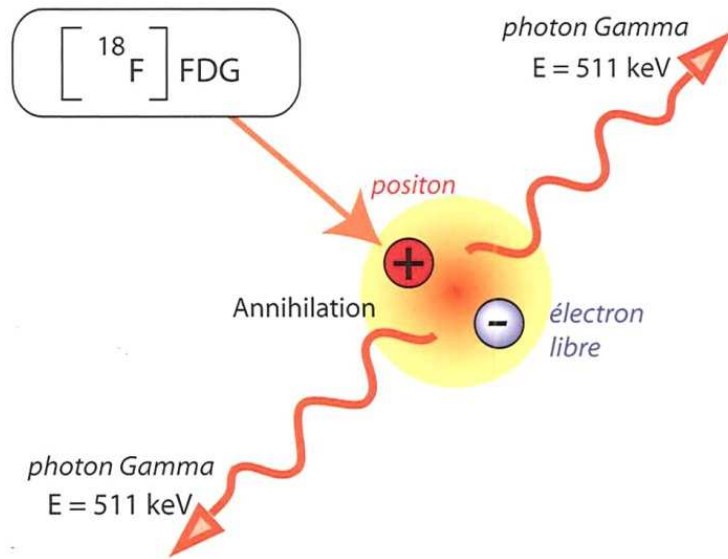
- Monte Carlo simulations (gold standard)
- Measured data



The way towards
Quantitatively accurate
SPECT imaging

PET/CT

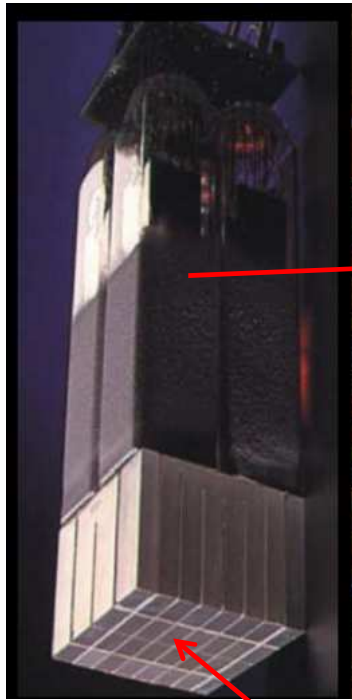
Basic principle of PET



Radionuclides used in PET : ^{11}C , ^{13}N , ^{15}O , ^{18}F , ^{68}Ga , ^{82}Rb

PET detector design

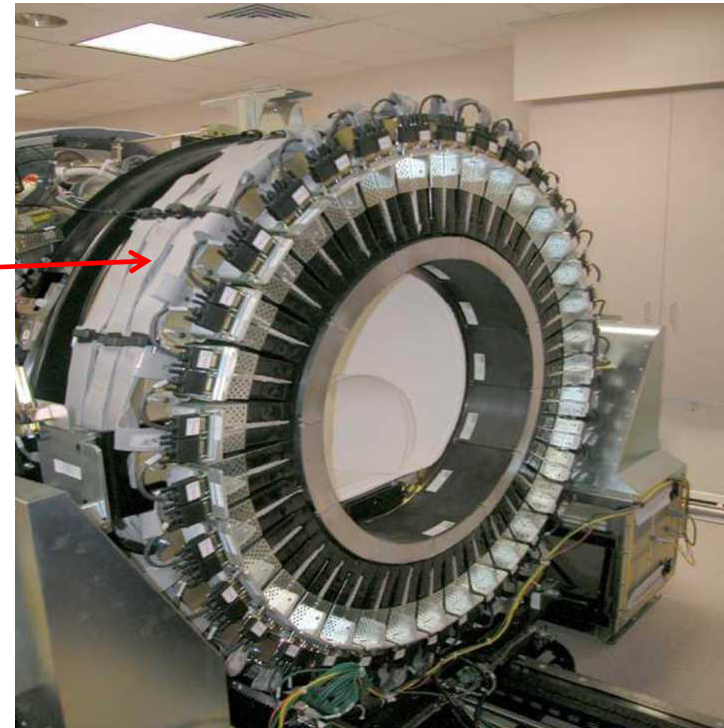
Modules



Bloc

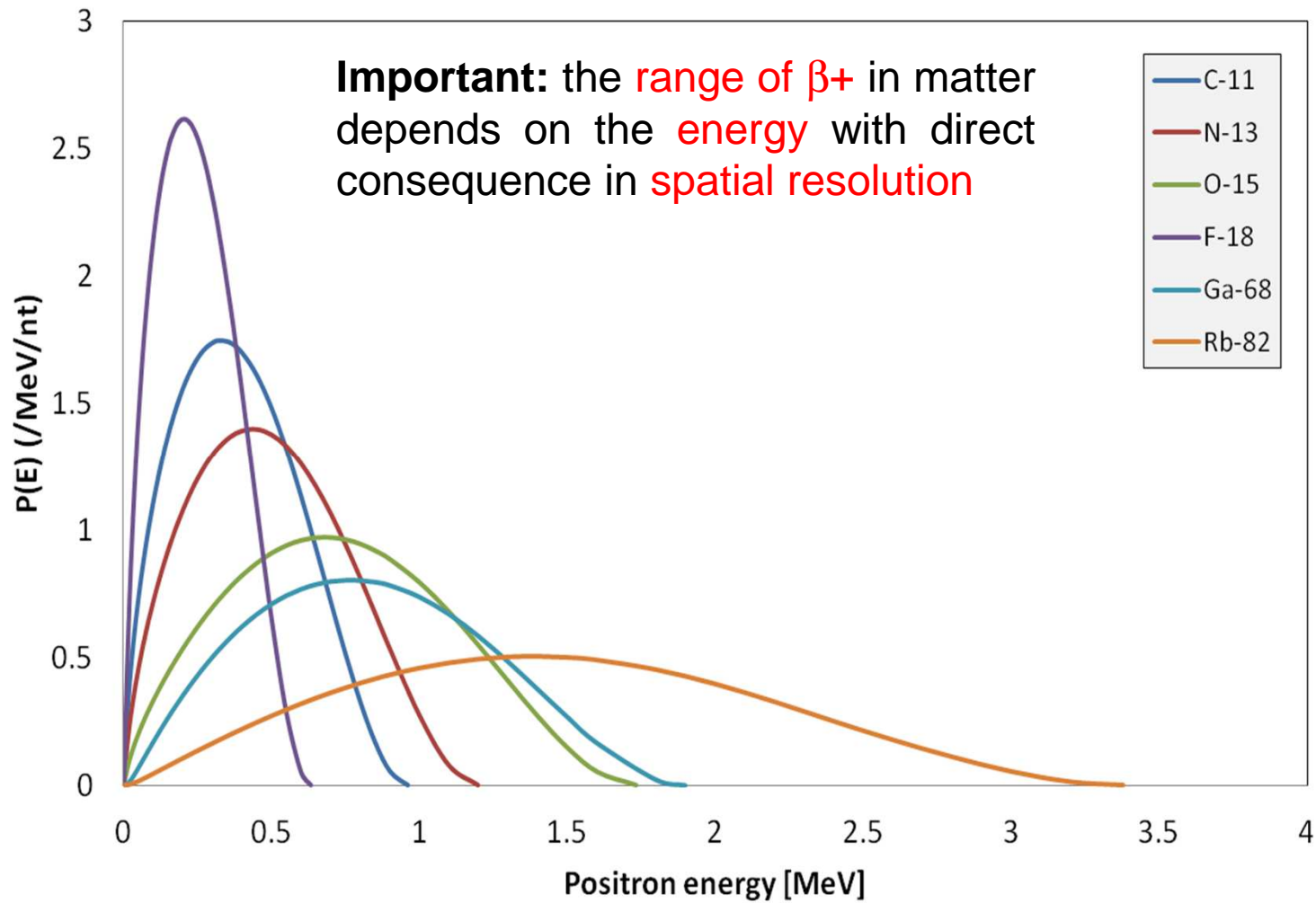


PET ring

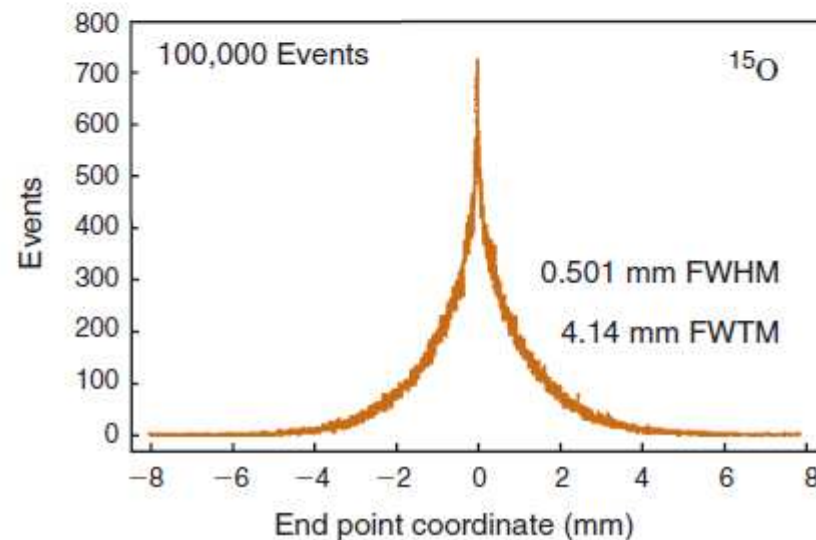
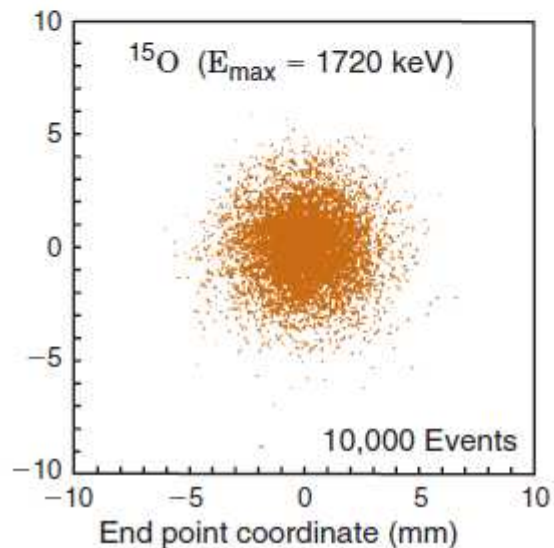
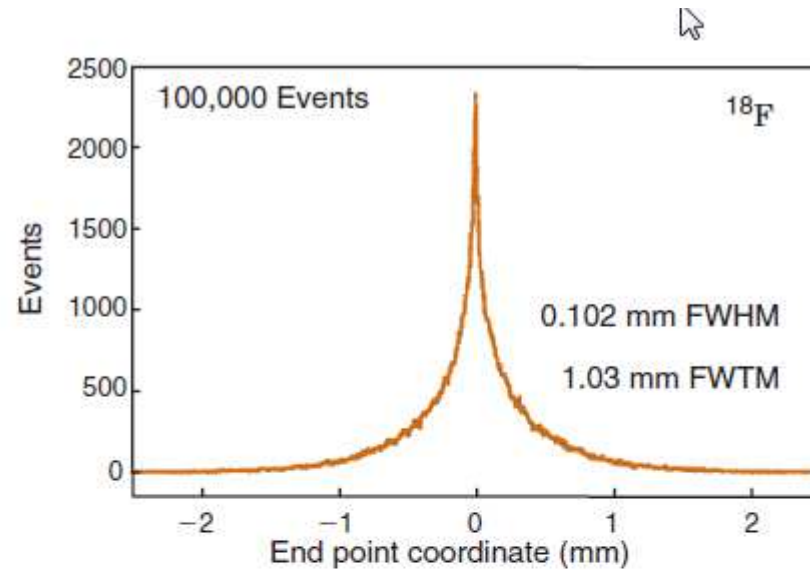
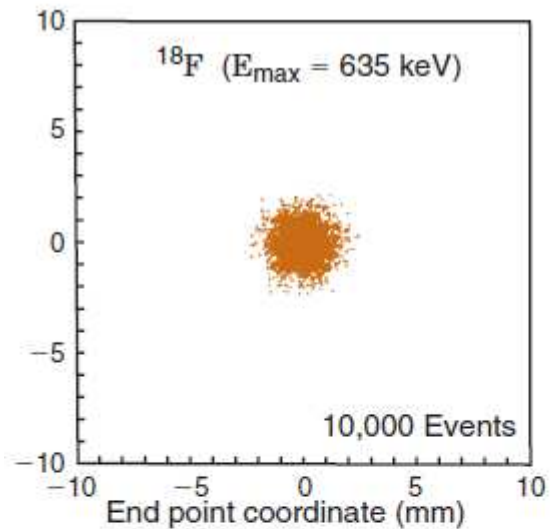


Detector elements (scintillators)

Energy spectra in β^+ decay

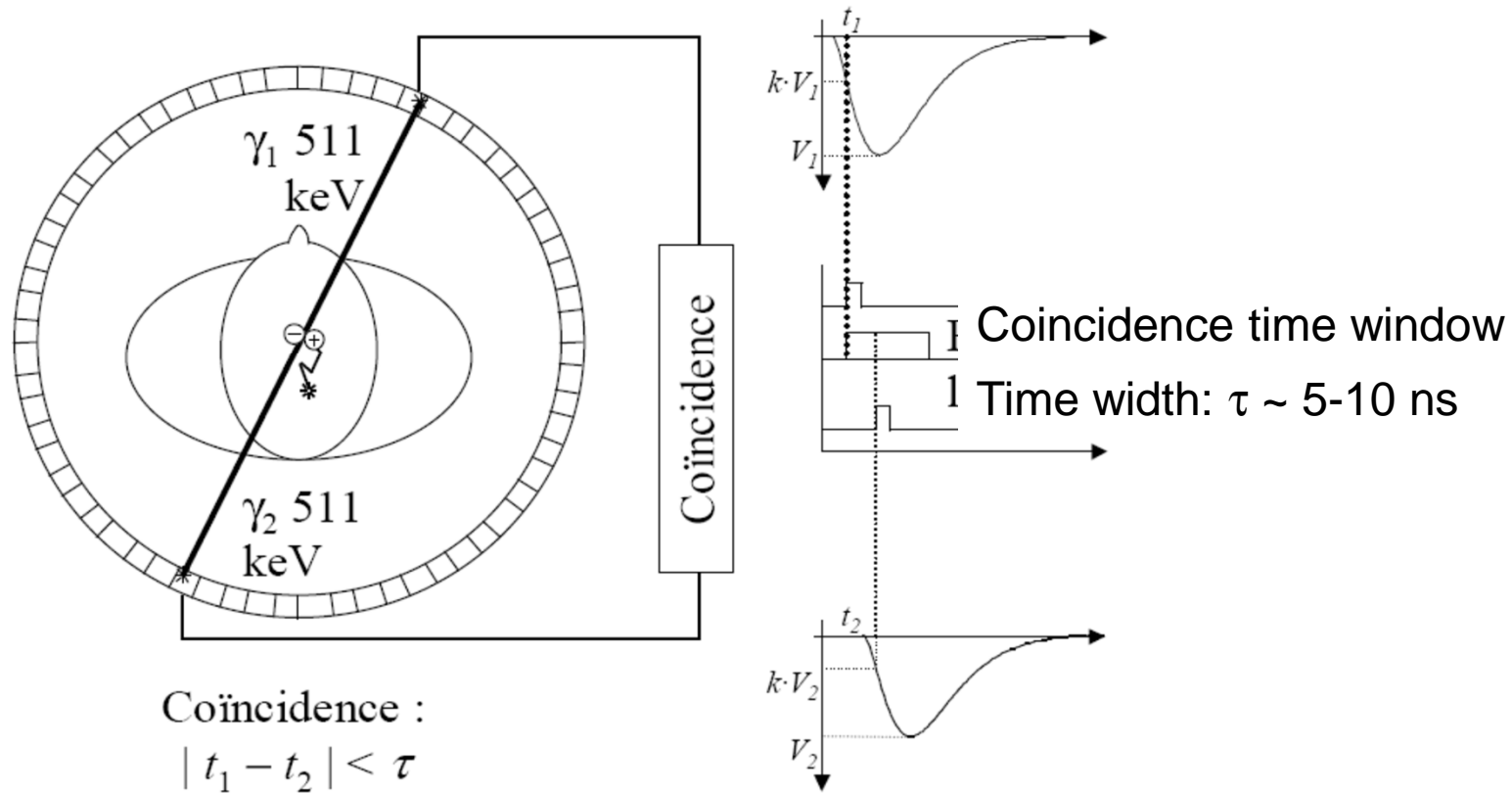


β^+ emission: Energy and range



Coincidence detection: Electronic collimation

Camera: Detector ring with detector blocs

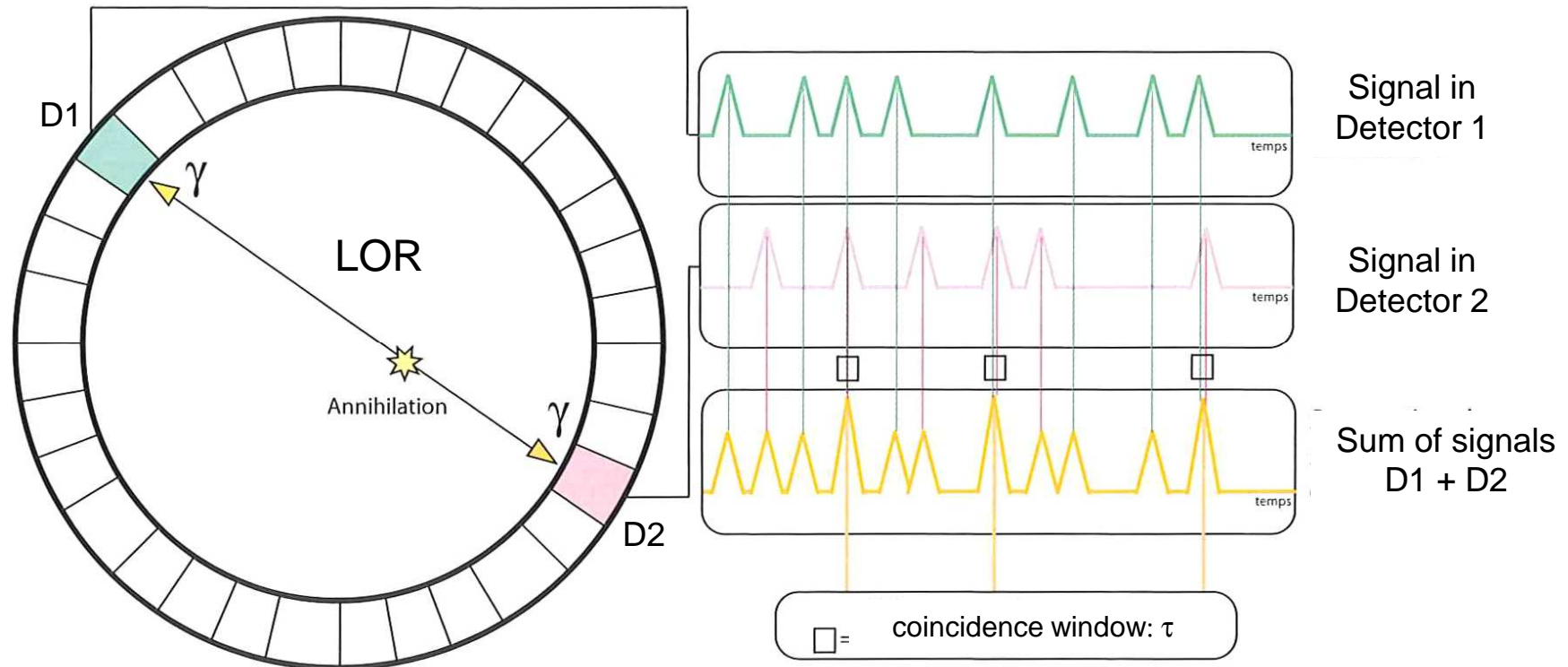


Coincidence are events couple of events

- occurring at the "same time" (\sim ns)
- having the right energy (\sim 511 keV each)

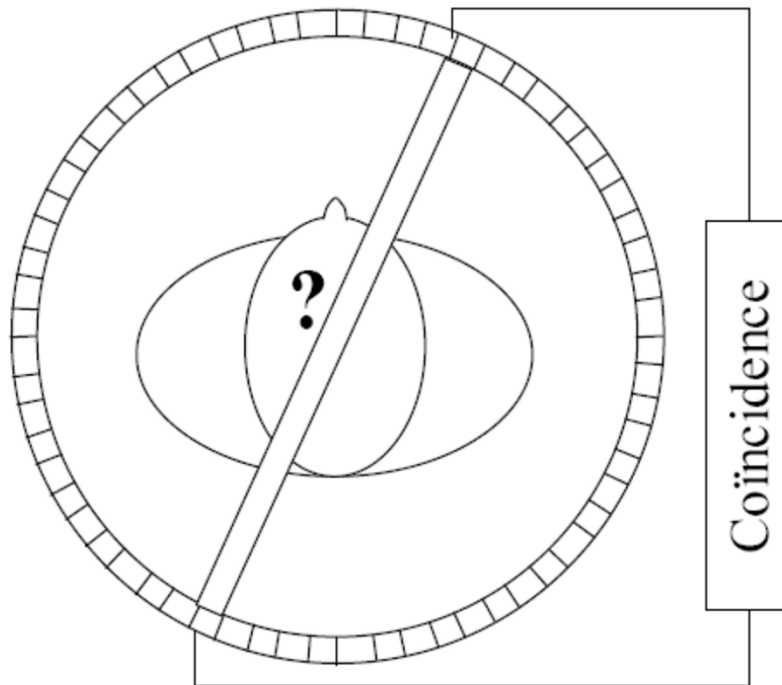
Coincidence detection

Only photons detected in coincidence are considered to build the image



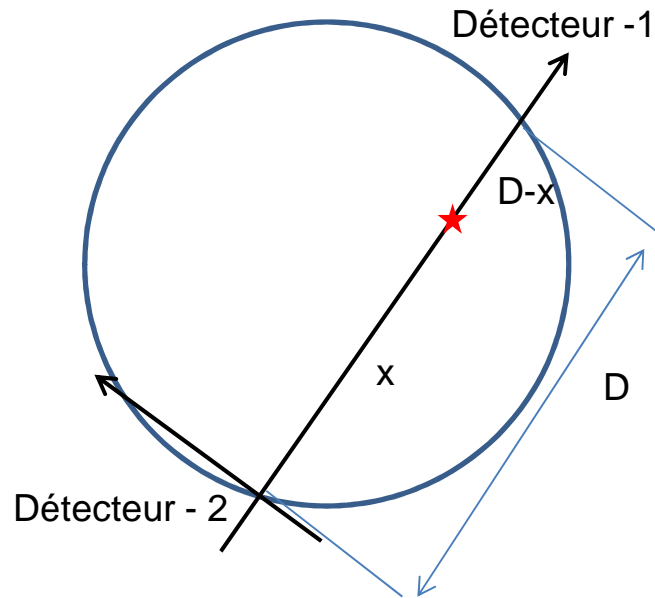
Spatial localization of annihilation events

2-511keV photon in coincidence → 1 Line (tube) Of Response (LOR)



- **Goal**
 - Recover the exact position of the annihilation event
- **Problem**
 - We have not information about the place along the LOR where the annihilation happened

Direct localization using the Time of Flight (TOF) information



Measured detection time in D1 and D2

$$T_1 = \frac{D-x}{c} \quad T_2 = \frac{x}{c}$$

$$\Delta T = T_2 - T_1 = \frac{x}{c} - \frac{D-x}{c} = \frac{2x-D}{c}$$

Uncertainty on time estimation \rightarrow
Error in annihilation position estimation

$$\delta T = \frac{\delta x}{c}$$

Direct localization using the Time of Flight (TOF) information

- **Source 1**

- $t_{\gamma_1} = D_1/c \rightarrow 1.4 \text{ ns}$

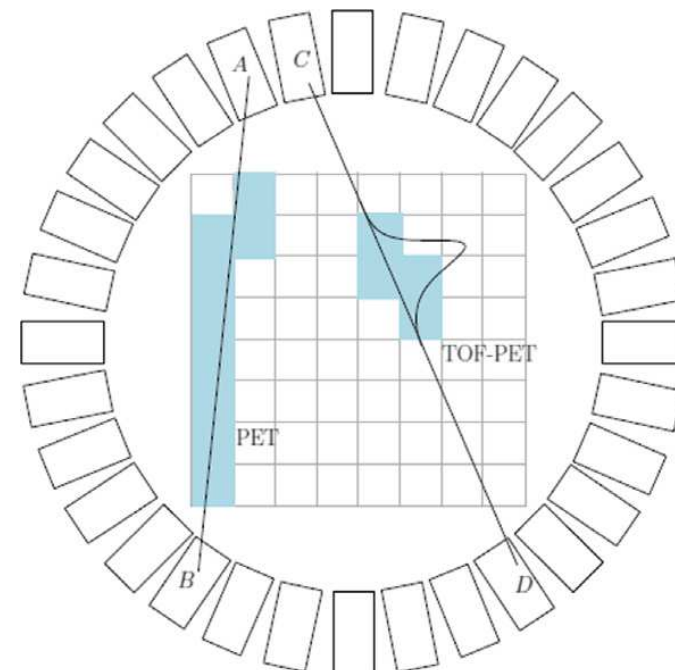
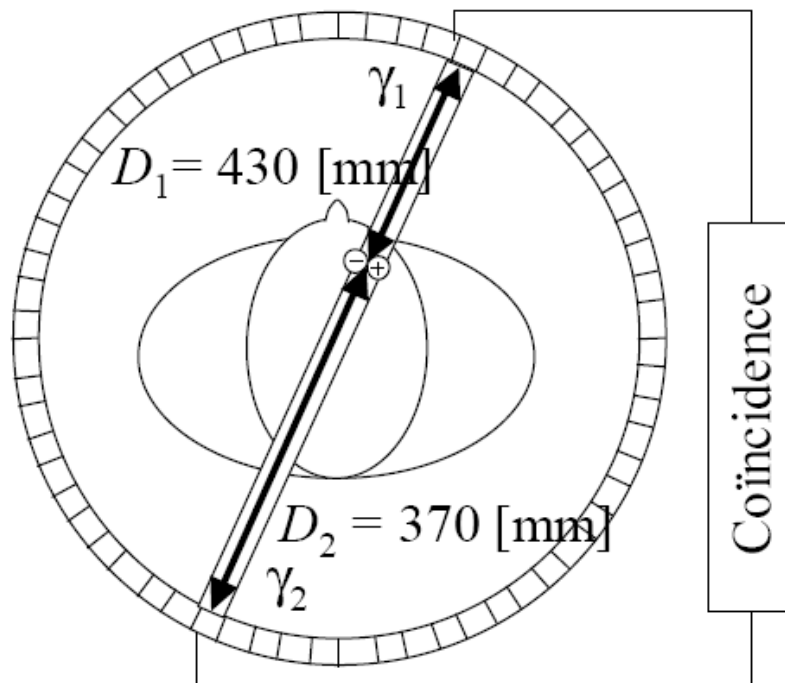
- **Source 2**

- $t_{\gamma_2} = D_2/c \rightarrow 1.2 \text{ ns}$

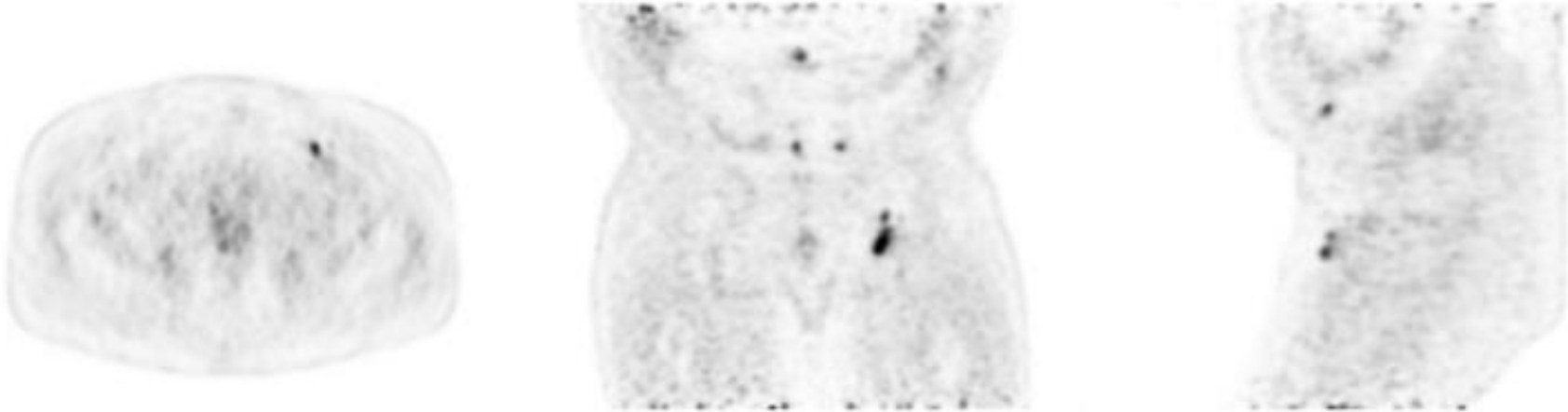
- Difference in time of flight $\Delta t = 0.2 \text{ ns} = 200 \text{ ps}$

$$c = 3 \cdot 10^{11} \text{ mm/s}$$

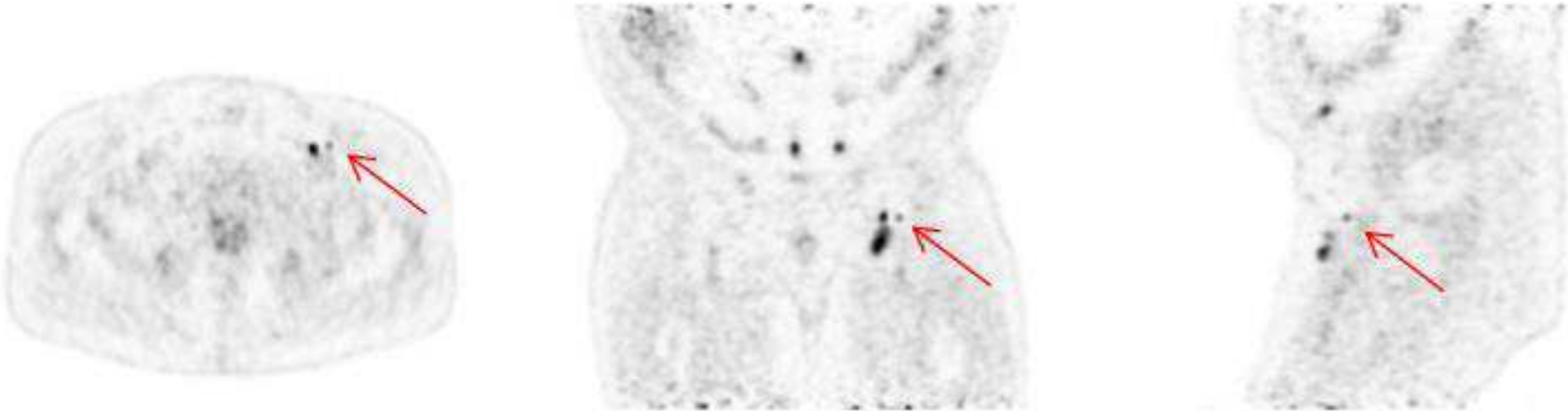
$$\Delta x = \frac{c\Delta t}{2} \Leftrightarrow \Delta t = \frac{2\Delta x}{c}$$



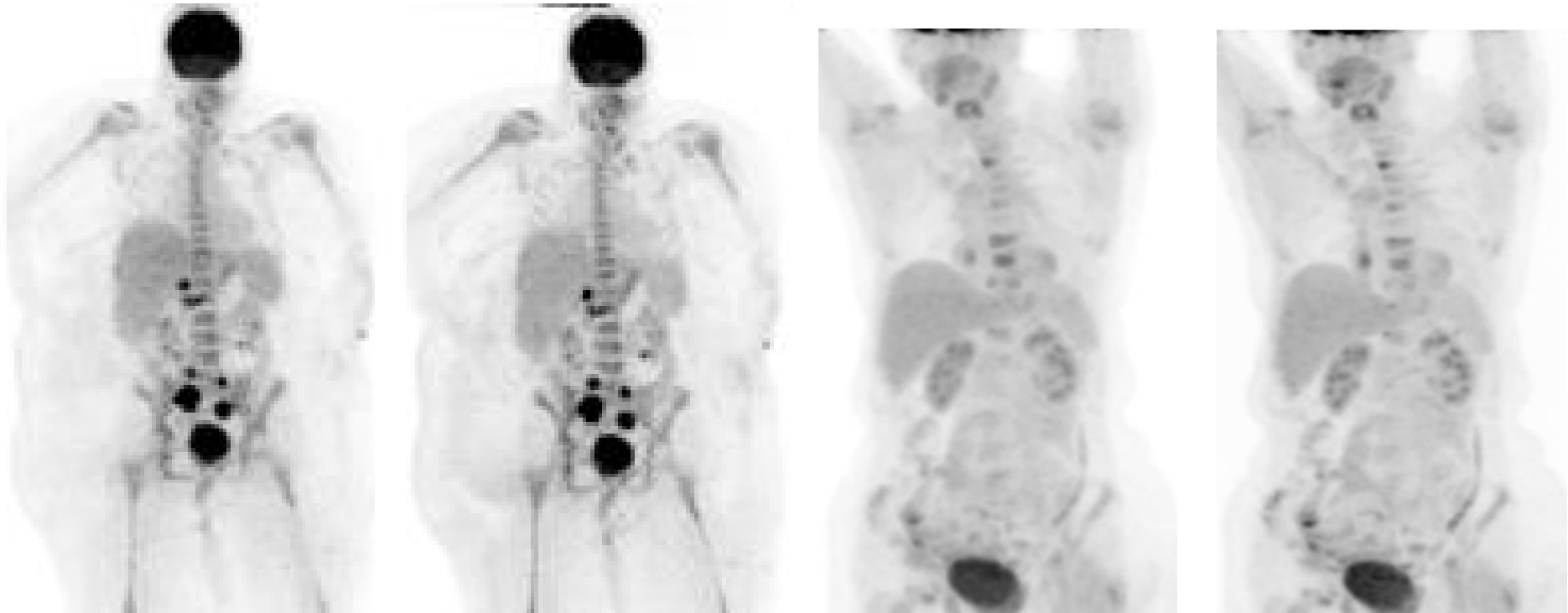
Improved pelvic nodule visualization with Time-of-Flight



Non-TOF

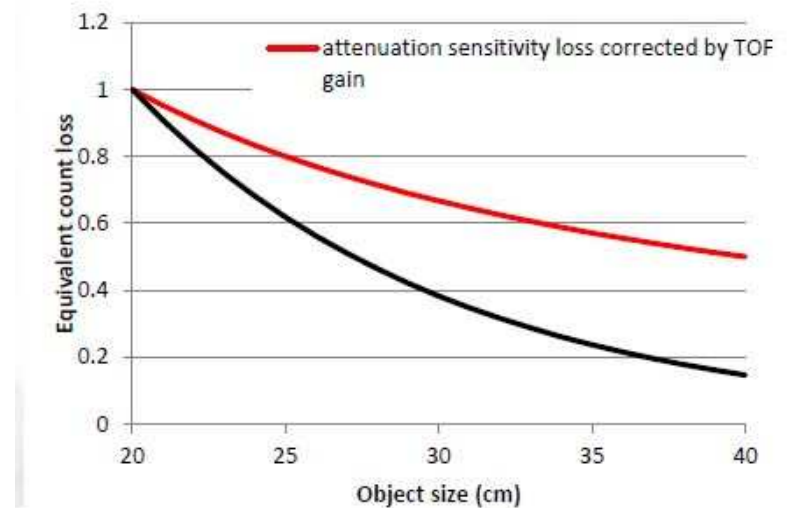


TOF



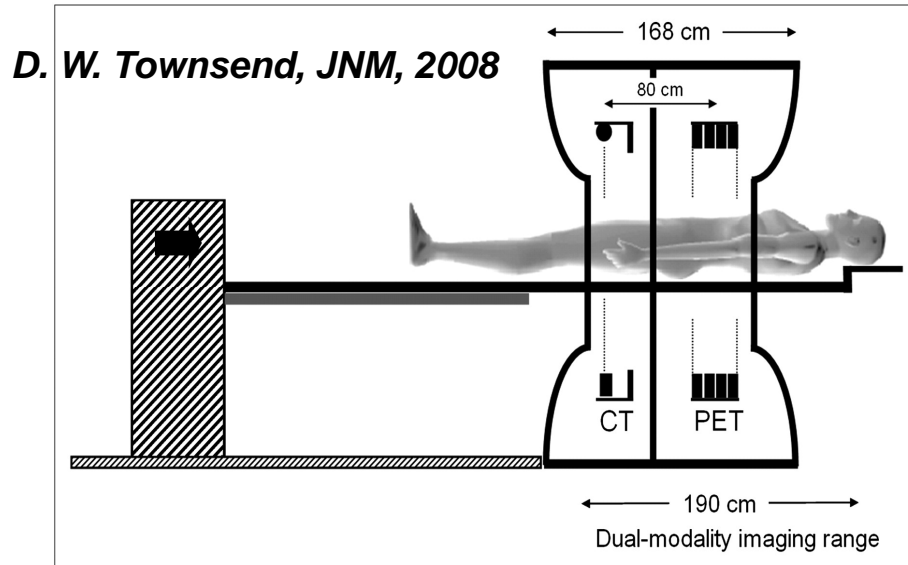
Gain based on: $Sensitivity_{gain} \propto 2 \times \frac{D(cm)}{\Delta t(ns) \times c}$

Body attenuation greatly reduces counts. As size increases, counts are reduced exponentially. ToF gain is greater for large patients as it partially compensates for the lower quality of large patients

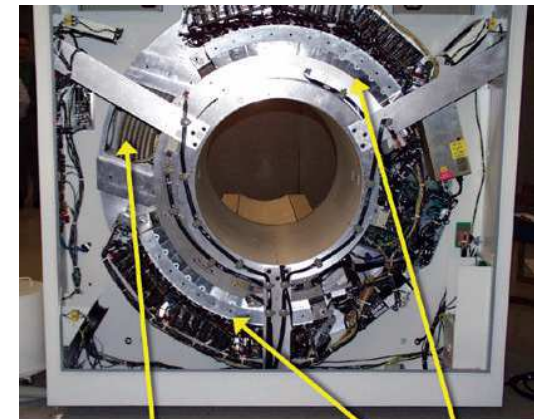


Dual modality PET-CT

- **Goal** : improve activity localization and implement attenuation correction (auto-registration of anatomic CT and functional PET)



X-ray tube X-ray detector

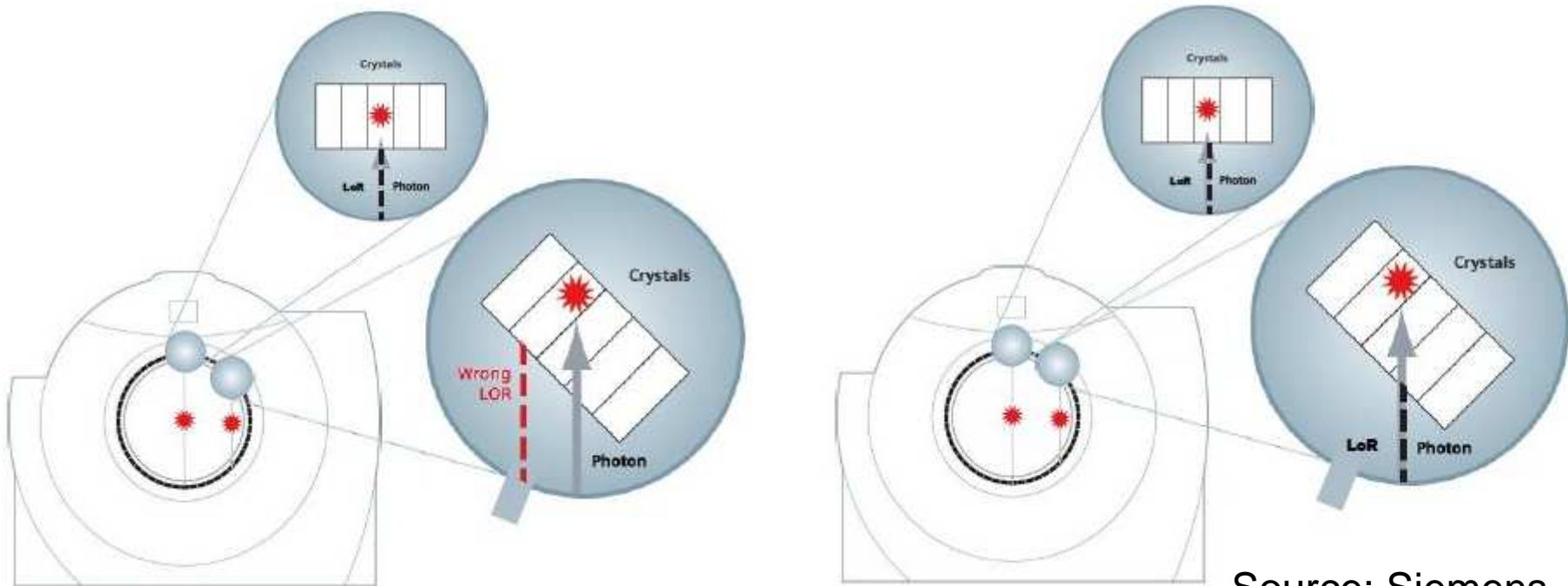


PET detector



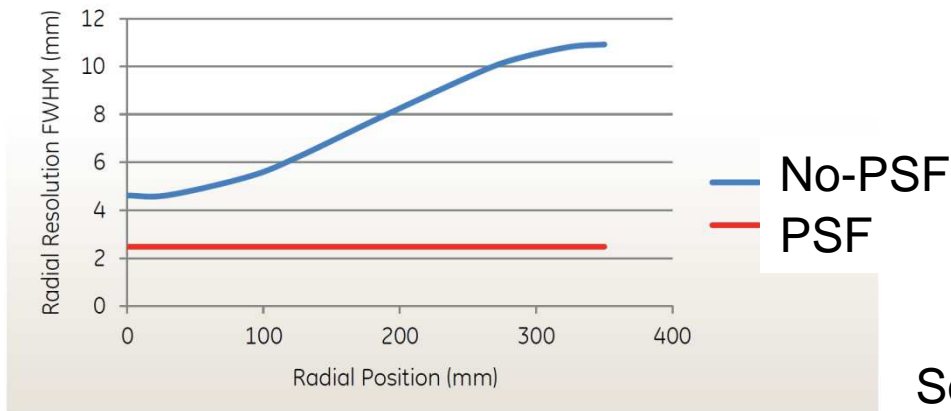
CT PET

Modeling of the PSF, improves actual positioning of the LoRs



Source: Siemens

PSF → uniform space resolution across the FOV



Source: GE

Spatial resolution

$$R_t = K_r \cdot \sqrt{R_i^2 + R_p^2 + R_a^2 + R_l^2}$$

- R_i is related to the detector width (w)
 - from $w/2$ (center) to w (detector), 2 – 4 mm
- R_p is related to the positron range
 - 0.2 mm for ^{18}F and 2.6 mm for ^{82}Rb
- R_a is related to the γ non-collinearity
 - $\pm 0.25^\circ$ deviation from 180°
 - 1.8 mm for a 80-cm PET scanners
- R_l is related to the localization of detector
 - (use of block detectors instead of single detectors)
 - 2.2 mm for BGO (less for LSO)
- K_r is a factor related to the reconstruction technique (1.2 to 1.5)
- R_t at the center of the FOV : 5 mm for ^{18}F

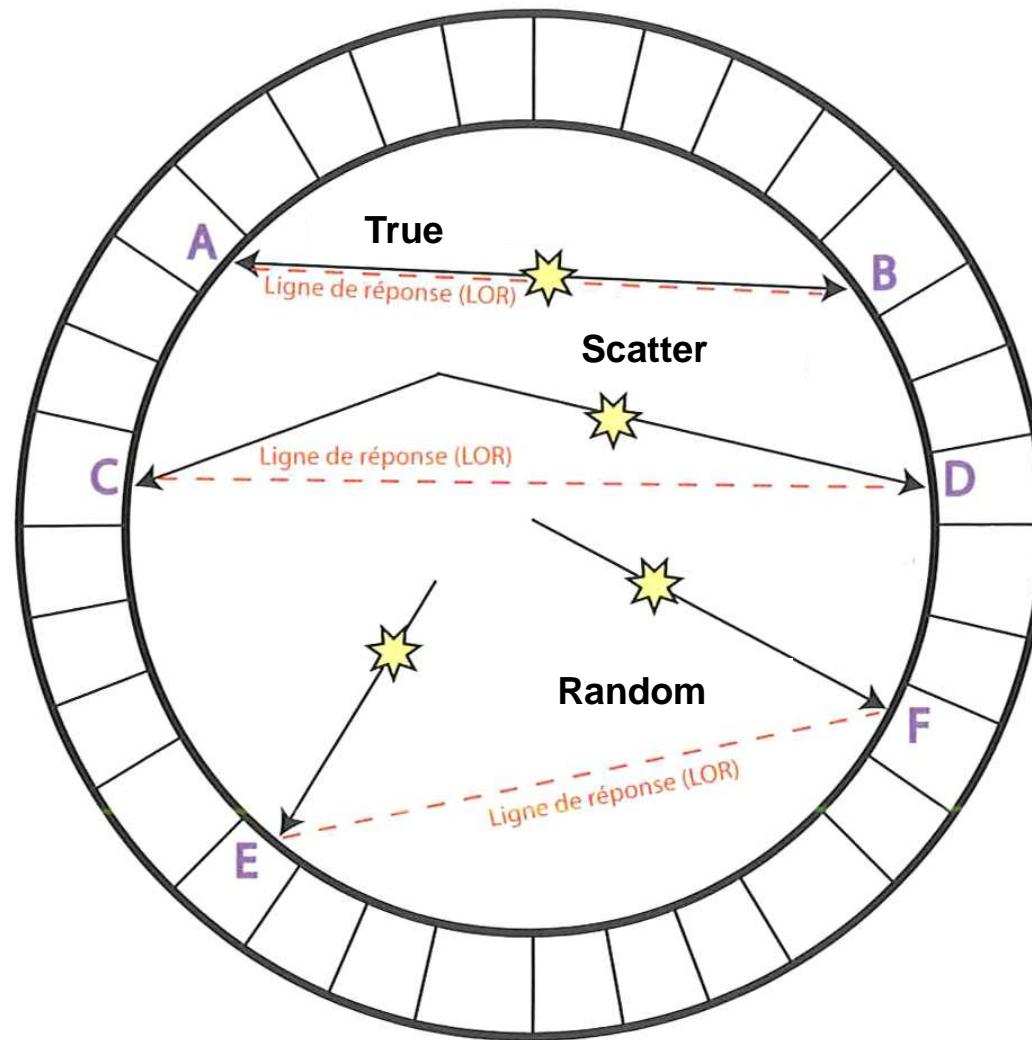


Detection efficiency

$$S = \frac{A}{4\pi r^2} \cdot \varepsilon^2 [\text{cps/MBq}]$$

- A = detector area seen by a point source to be imaged
- $\varepsilon = 1 - \exp(-\mu x)$ detector's efficiency
- μ = linear attenuation coefficient of 511 keV photons in the detector
- x = thickness of the detector
- r = radius of the detector ring
- $S = 0.2 - 0.5\%$ for 2D PET and 1-10% for 3D PET
($S = 0.01-0.03\%$ for SPECT)
- Manufacturer provides volume sensitivity S_{vol} [cps/Bq/ml]

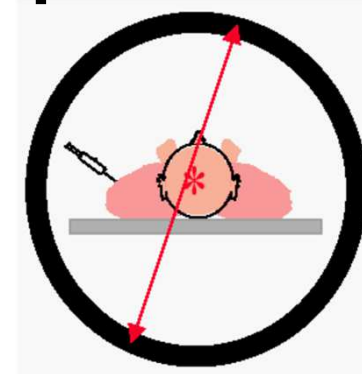
Coincidence event type in PET



Coincidence event type in PET

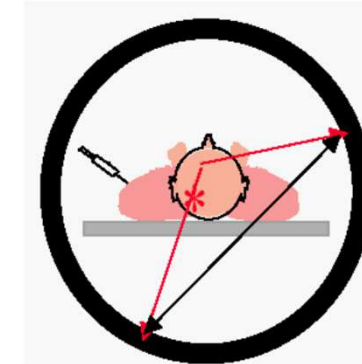
- **True coincidence**

- ☞ Correct localization long the LOR
- ☞ Useful for image reconstruction



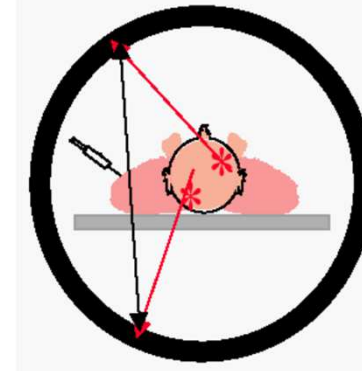
- **Scatter coincidence (Compton)**

- ☞ Mislocalization
- ☞ Contrast reduction
- ☞ Quantitative bias



- **Random coincidence**

- ☞ Mislocalization
- ☞ Important component → count rate saturation
- ☞ Quantitative bias



Corrections for Quantitative Studies : All PET is (almost) Quantitative !

Raw Sinogram Data (Trues + Scatters + Randoms)

Remove Randoms

Normalize Detector Responses

Correct for Deadtime

Correct for Scatter

Correct for Attenuation

It's not exactly like
this, and it's not
necessarily as linear as
this!

**T Sinogram
Ready for Reconstruction**

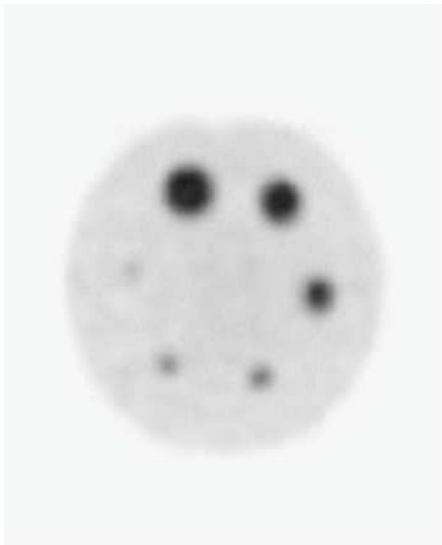
PVE correction

Recovery coefficient (RC)

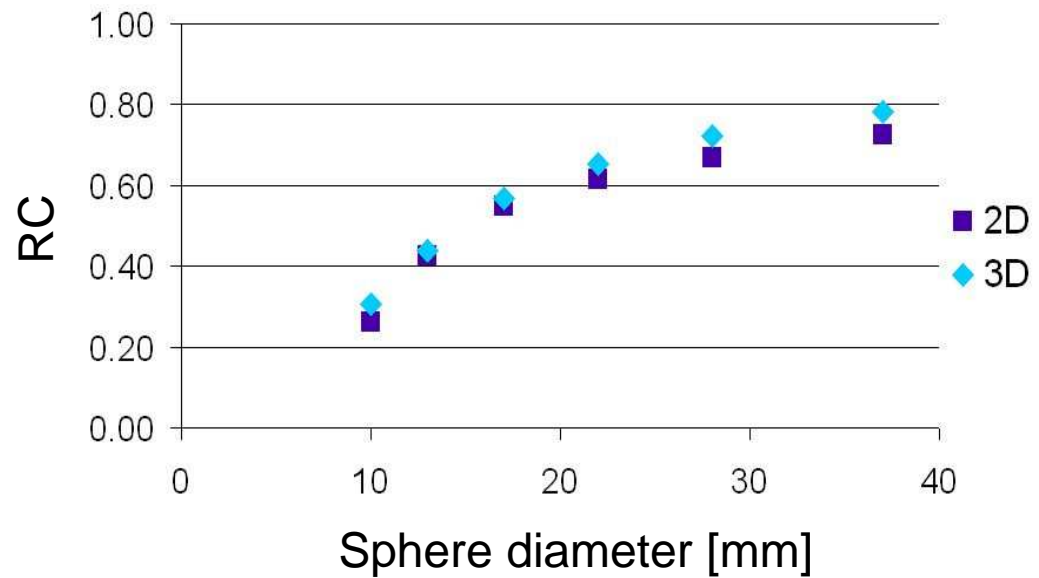
$$RC = \frac{\text{Observed activity concentration}}{\text{True activity concentration}}$$



$$A_{\text{corrected}} = \frac{A_{\text{measured}}}{RC}$$



^{18}F (GE Discovery LS)



Specific Uptake Value (SUV) concept

$$\text{SUV} = \frac{\text{Measured Activity Concentration [Bq/ml]} \times 10^3}{\left[\frac{\text{Injected Activity* [Bq]}}{\text{Patient Mass [kg]}} \right]}$$

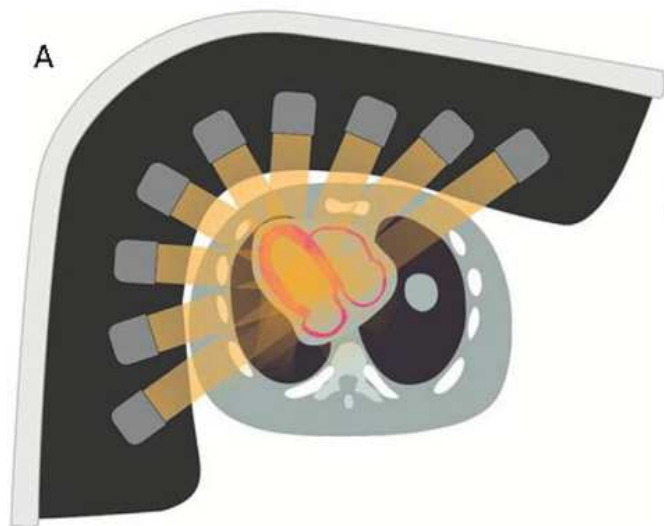
** Reported
at the
beginning of
the exam*

**SUV = semi-quantitative index of the ^{18}F FDG accumulation \Rightarrow
makes possible the comparisons between exams**

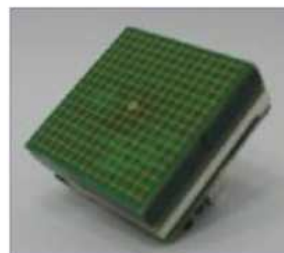
- ❖ SUV is used as an index to determine if a hotspot is significant
- ❖ Its use depends on :

Time between injection and acquisition, patient's blood sugar level, patients's weight, quantification quality (attenuation correction, ...), partial volume effects, ...

Recent developments

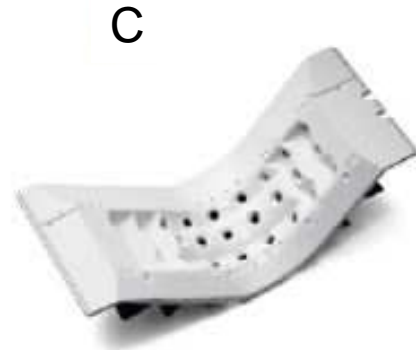
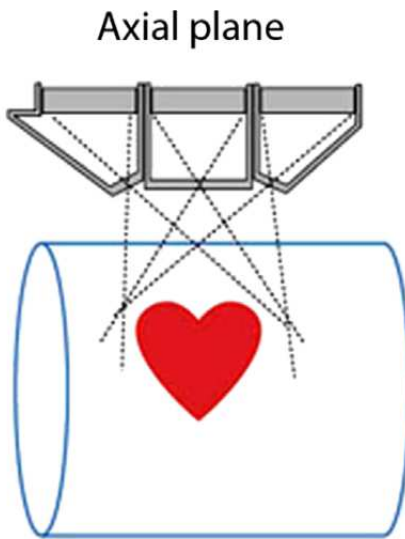
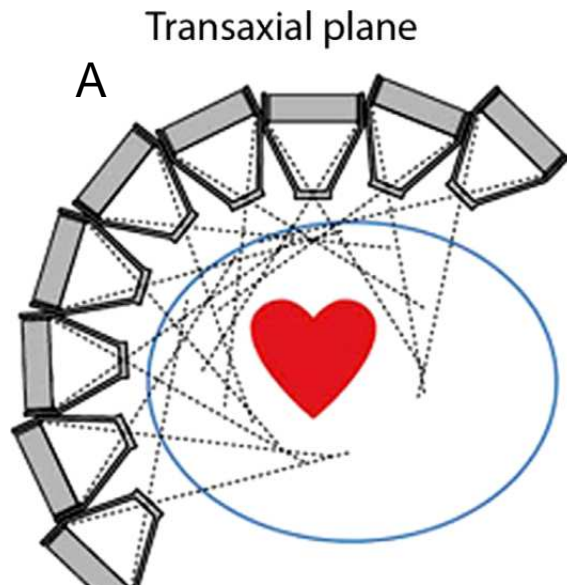


**Semi conductor
gamma camera
Cardiac Gamma
camera**



New collimators and
acquisition geometry

Acquisition geometry of the D-SPECT system with 9 detector blocks (A). Photograph of the camera (B), 1 detector column (C), and 1 CZT detector element (D). (SpectrumDynamics)



Acquisition geometry of the GE NM 530c multipinhole system (A). Photograph of the camera (B), multipinhole collimator (C)



The **CZT-SPECT-camera** (pixelated detector of a size of 2.46 mm/pixel and energy resolution of 6.3% compared to an energy resolution of 9.8% for the NaI-camera)

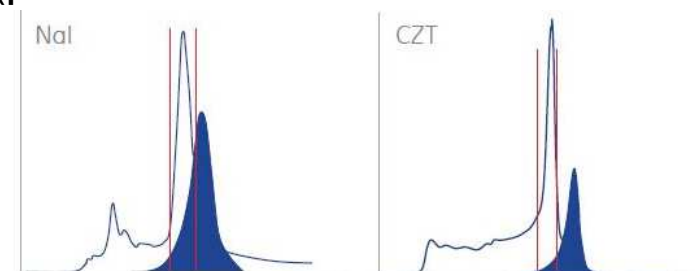
Better energy resolution → reduce scatter contribution

Higher spatial resolution ~ 3mm

Higher count rate achievable

Higher sensitivity

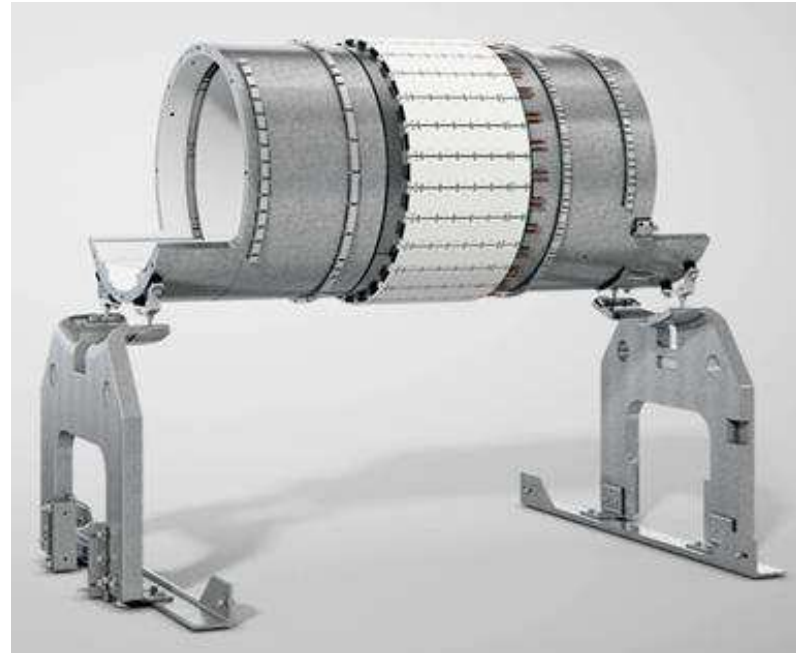
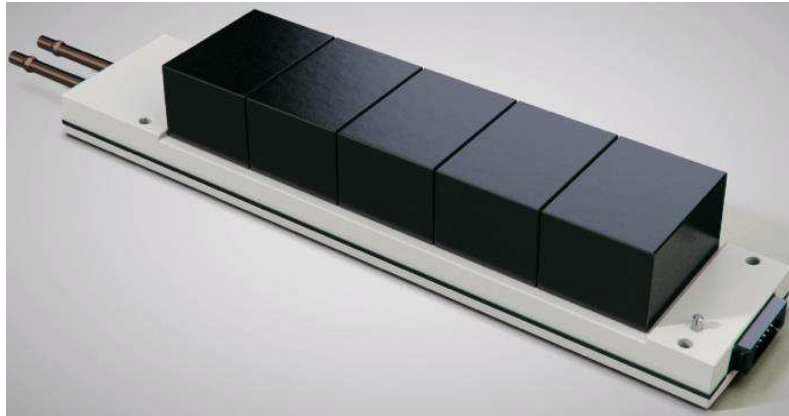
→ Shorter acq. time and/or low administered activity (patient dose reduction)



Overlay of ^{99m}Tc and ^{123}I spectra, showing greater crosstalk between the two peaks for the NaI detector with its poorer energy resolution and wider energy window.

Source: GE

Semiconductor based (SiPM) PET



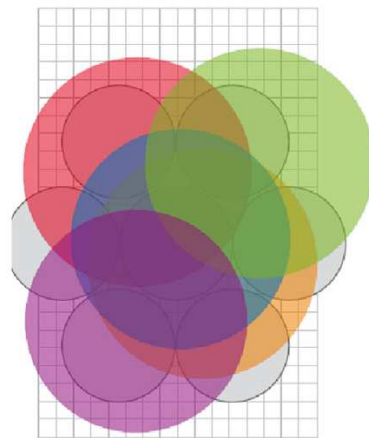
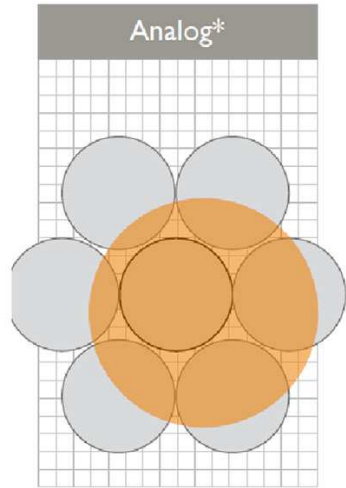
Detector modules developed to operate in high magnetic field
(PET/MRI)

Source: GE

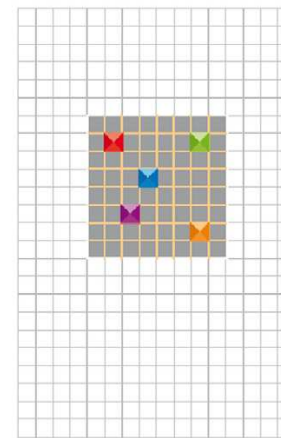
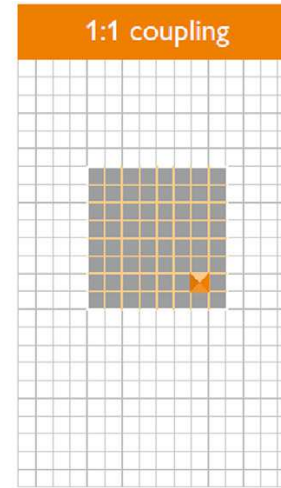
SiPM



Conventional PM



Semiconductor SiPM



Improved signal localisation
Improved space resolution

Decreased signal Pile-up
Higher count rate achievable

Source: Philips

Conventional vs. SiPM PET

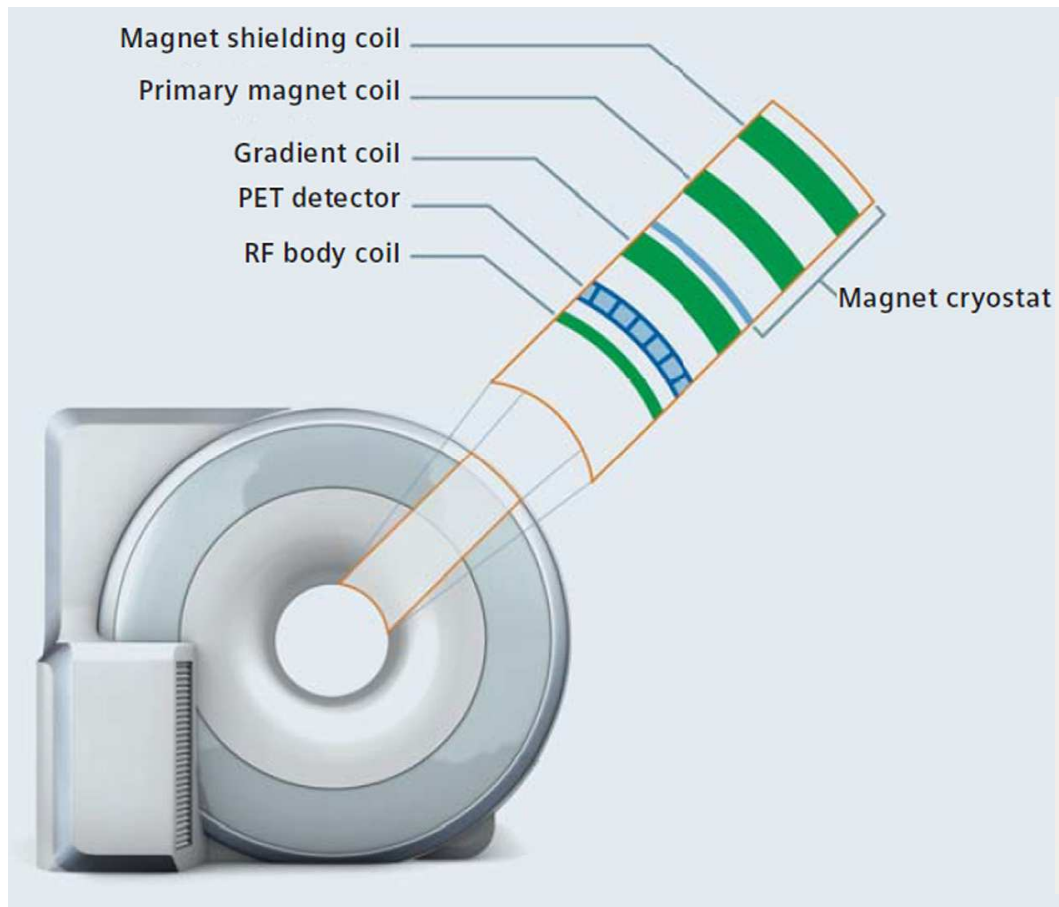
Table – Comparison of the Philips Ingenuity TF, GE Discovery 710, Biograph mCT Flow and the new Philips digital PET/CT Vereos.

Model Product Name	Ingenuity TF	Discovery 710	Biograph mCT Flow	Vereos
Patient port [cm]	70 OpenView	70	78	70
Patient scan range [cm]	190	200	195	190
Maximum patient weight [kg (lb)]	195 (430)	226 (500)	226 (500)	195 (430)
Acquisition modes	3D S&S	3D S&S	3D S&S, continuous	3D S&S
Number of image planes	45 or 90	47	109	72
Plane spacing [mm]	2 or 4	3.27	2	1, 2, or 4
Crystal size [mm]	4 × 4 × 22	4.2 × 6.3 × 25	4 × 4 × 20	4 × 4 × 22
Number of crystals	28,336	13,824	32,448	23,040
Number of PMTs	420	256	768	23,040 SiPMs
Physical axial FOV [cm]	18	15.7	21.8	16.3
Detector material	LYSO	LYSO	LSO	LYSO
System sensitivity 3D, [%] [*]	0.74	0.75	0.95	>1.0
Trans axial resolution @ 1 cm [mm] [*]	4.7	4.9	4.4	4.0
Trans axial resolution @ 10 cm [mm] [*]	5.2	5.5	4.9	4.5
Axial resolution @ 1 cm [mm] [*]	4.7	5.6	4.5	4.0
Axial resolution @ 10 cm [mm] [*]	5.2	6.3	5.9	4.5
Peak NECR [kcps]	120 @19 kBq/ml	130 @29.5 kBq/ml	175 @28 kBq/ml	400 @30 kBq/ml
Time-of-flight resolution [picoseconds]	591	544	540	307
Time-of-flight localization [cm]	8.9	8.2	8.1	4.6
Coincidence window [nanoseconds]	4.5	4.9	4.1	1.5

The sensitivity, NECR (noise equivalent count rate), coincidence window and TOF resolution are higher for the digital PET/CT digital PET/CT.
 Abbreviations: FOV, field-of-view; PMT, photomultiplier tubes; NECR, noise equivalent count rate; kcps, kilocounts per second; kBq/ml, kiloBecquerel/milliliter; S&S, step and shoot.

^{*} NEMA 2001.

PET / MRI



Source: Siemens